CZECH UNIVERSITY OF LIFE SCIENCES PRAGUE

Czech University
of Life Sciences Prague

FACULTY OF ENVIRONMENTAL SCIENCES

Department of Spatial Sciences

USE OF POINT PATTERNS TO MODEL DISTRIBUTION OF 2021 BRITISH COLUMBIA WILDFIRES

Diploma Thesis

Thesis Supervisor: *D.Sc. Olga Špatenková*

Author: *Bc. Polina Moisseyenko*

Prague

2023

CZECH UNIVERSITY OF LIFE SCIENCES PRAGUE

Faculty of Environmental Sciences

DIPLOMA THESIS ASSIGNMENT

Bc. Polina Moisseyenko

Engineering Ecology
Nature Conservation

Thesis title

Use of point patterns to model distribution of 2021 British Columbia wildfires

---

Objectives of thesis

This thesis aims to analyze and model the distribution of forest fires in British Columbia that occurred in summer 2021. Within the framework of Point Patterns, it aims to identify significant factors influencing the occurrence of the fires and explore the corresponding spatial and temporal scales. The observed results will be used to fit a suitable point process to the data.

Methodology

The ignition of forest fires can be regarded as point patterns distributed along the study area characterized by first-order effects (intensity) and second-order effects (point interactions). These measures unveil possible spatial dependency and clustering in the data that help us understand the underlying processes and fit a suitable model. The author will thoroughly interpret the observed results and discuss their usefulness.

The proposed extent of the thesis

40-50 pages

Keywords

Suitable keywords will be selected by the author.

Recommended information sources

AFTERGOOD, O.S.R., FLANNIGAN, M.D. 2022. Identifying and analyzing spatial and temporal patterns of lightning-ignited wildfires in Western Canada from 1981 to 2018. Canadian Journal of Forest Research. 52(11): 1399-1411.

ARAGÓ, P., JUAN, P., DÍAZ-AVALOS, C. et al. 2016. Spatial point process modeling applied to the assessment of risk factors associated with forest wildfires incidence in Castellón, Spain. Eur J Forest Res 135, 451–464.

TURNER, R. 2009. Point patterns of forest fire locations. Environ Ecol Stat 16, 197–223

Expected date of thesis defence

2022/23 SS – FES

The Diploma Thesis Supervisor

D.Sc. Olga Špatenková

Supervising department

Department of Spatial Sciences

Electronic approval: 28. 2. 2023

doc. Ing. Petra Šímová, Ph.D.

Head of department

Electronic approval: 1. 3. 2023

prof. RNDr. Vladimír Bejček, CSc.

Dean

Prague on 02. 03. 2023

Declaration

I have worked on my diploma thesis titled “Use of patterns to model distribution of 2021 British Columbia wildfires” by myself, and I have used only the sources mentioned at the end of the thesis. As the author of this diploma thesis, I declare that my work does not break any other person's copyrights.

In Prague on _____ Bc. Polina Moisseyenko

Acknowledgements

I would like to sincerely thank my supervisor, D.Sc. Olga Špatenková, for her academic guidance, encouragement, and patience through the elaboration of this thesis. I would like to express my gratitude to my family and companions for their unlimited support and inspiration.

Abstract

This diploma thesis deals with wildfires in boreal forests. Wildfires are one of the most frequent sources of tree cover loss in boreal forest regions. The pattern of wildfires has been changing globally.

The author of this diploma thesis is aimed to evaluate the pattern of wildfires that occurred in British Columbia during the 2021 wildfire season in terms of 1st and 2nd order effects. The chosen external factors (mean wind speed, distance from roads, vegetation zones, and average drought level) were considered during the calculations. The results show that the distribution of wildfires had a clustering pattern in the southern parts of the province. All of the considered factors are associated with wildfire incidents. The author attempted to model the relationship between wildfire incidents and external factors. The final model was used to visualize a prediction of wildfires throughout the study area. The prediction was further compared to the wildfire events that occurred one year later. These results highlight that point pattern analysis of wildfire incidents can be used to predict areas of high wildfire risk.

Keywords: wildfires, kernel density, L-function, G-function, Poisson process

Table of Contents

1. Introduction

According to the World Resources Institute and Global Forest Watch, during the last two decades, wildfires caused a tree cover loss of 91 million hectares globally (Khakzad, 2019). Across the world biomes, boreal forests in North America and Eurasia are associated with the highest area of forest loss related to wildfire during 2001-2019 (Tyukavina et al., 2022a). Fire is considered a natural process in boreal forests, shaping its diversity and biochemical cycles, and takes part in the natural succession cycle. Dry forest fuels and winds represent the essential elements in large wildfire events. Boreal forests have already been experiencing drying caused by human-caused climate change during the last decades, which will expectedly enhance the frequency and severity of wildfires (Girardin et al., 2010). A study by Tyukavina et al. has already detected an increasing trend of forest loss area related to wildfire in boreal forests of the Eurasian region.

The combined effects of human development and climate change are expected to result in increasing in wildfire events and severity. It was projected that raising global temperature increases the number of lightning that represents one of the main sources of wildfires. Increased human activities in wildlands as well contribute to a higher likelihood of ignition (Khakzad, 2019).

It is seen that the interest in the problematics of wildfires especially has increased during the era of changing climate. Understanding past fire activity and natural disturbance regime is essential for predicting future fire events that, therefore, is crucial for the development of forest management policies, better estimation of future carbon balances, resilience, and mitigating the effect of the changing climate (Girardin et al., 2010).

There are scientific papers that are discussing the wildfire problematics within both the northern and southern hemispheres. Authors of these papers study past wildfires, construct spatial patterns of the wildfires, and aim to predict future wildfire events. A crucial part of their methodology is a point pattern analysis (Vadrevu & Badarinath, 2009; Aragó et al., 2016; Aftergood & Flannigan, 2022).

The wildfire season 2021 in British Columbia was most certainly influenced by extreme heat waves indicating the below-average received precipitation (Coogan et al., 2022). As a result, the extreme heat and drought provoked an earlier beginning of wildfire season that recorded more than 1 500 wildfires (Province of British Columbia, 2022).

An increasing trend of wildfire events and the application of point pattern analysis to study wildfire patterns represent this thesis's primary sources of inspiration. In this work, wildfire distribution will be studied in terms of the 1st and the 2nd order effects – whether the distribution is influenced by underlying property or by the presence of other wildfires (Gimond, 2018).

2. Main objectives of the study

This study aims to analyze the pattern of the wildfires that occurred in British Columbia during the 2021 wildfire season. The first part of the thesis intends to comprehensively review the literature concerning wildfire problematics, trends in boreal forest loss, and connection to climate change. The literature review will also review the scientific papers addressing the problematics of wildfire study.

The description of the study area and the studied wildfire season, methodology, and point pattern analysis of the wildfires represent the second part of the work. The goal of the point pattern analysis is to explore the pattern in terms of 1st and 2nd order effects and to determine whether the pattern of the events is clustered or random. In addition, the analysis will be adjusted to consider external factors (mean wind speed, distance from roads, vegetation zones, average drought level) that may influence the pattern of the wildfires. The author will attempt to model the trend of wildfires within the region.

3. Wildfire problematics

3.1 Global trends

Forest loss or tree cover loss is defined as the complete removal of tree cover canopy (Hansen et al. 2013). Global tree cover loss during the years 2001-2021 in total was 434 million hectares. The four most dominant drivers of tree loss include forestry, commodity-driven deforestation, wildfires, and shifting agriculture. (Global Forest Review, 2022)

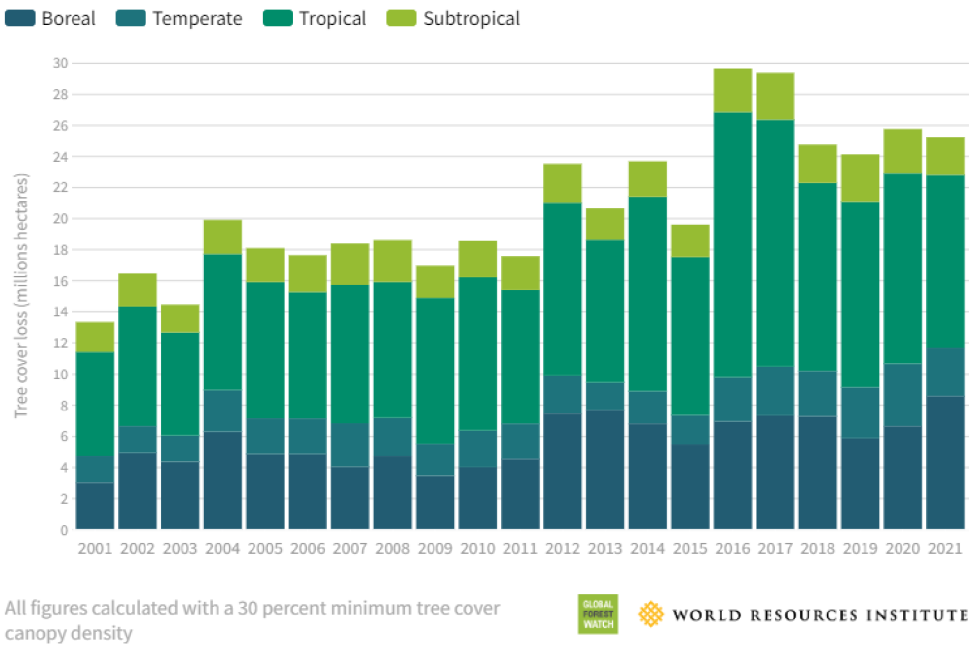

Fugure 1: Global tree cover loss between the years 2001 and 2021. Source: Global Forest Review, 2022.

A plot from Figure 1 shows that 11.12 mil ha of tree cover was lost in tropical forests during 2021. That represents around 42% of total tree cover loss. Deforestation in the tropics is mainly associated with agriculture and urbanization (Global Forest Review, 2022). In tropical rainforests, wildfires do not occur naturally. Hence fires are associated with human activities. Wildfires in tropical forests are connected to deforestation of the land for future conversion to oil palm and other plantation crops. A recent publication from R. Trancoso posits that the conversion practice might increase the risk of wildfires by four times within the 15-year period. (Trancoso et al., 2022).

According to Tyukavina et al., 2022 global trend of forest loss during 2001-2019 estimated that 26-29% of global forest loss was associated with wildfire. Contrary to tropical forests, fires in boreal forests are considered a natural process and participate in ecosystem dynamics (Tyukavina et al., 2022a). According to Global Forest Review, 97 % of tree cover loss in boreal forests was associated with forestry and wildfires.

Cumulative tree cover loss in Canada, Russia, and the United States represents 99% of loss in boreal forests related to wildfires. Even though tree cover loss caused by wildfires and forestry is considered temporary, the time needed for the regeneration of forests is variable and can last long. (Global Forest Review, 2022)

3.2 Wildfire trends in forests of Northern America and Eurasia

As it was mentioned in section 3.1, the most frequent causes of forest loss in boreal regions are wildfires and forestry (Global Forest Review, 2022). During the last decades, the world has been exposed to the changing climate, extended hot seasons, and increased frequency of severe wildfires. These fires have resulted in significant negative consequences in environmental, economic, and social areas. (Haghani et al., 2022)

According to the data from Global Forest Watch, in 2021, Russia, Canada, and the United States had the highest fire-related tree cover loss (Figure 2). The total fire-related loss in these countries is 7.8 million hectares; this corresponds to 84% of all tree cover loss due to fire in 2021 (Richter et al., 2022). A study of global trends of forest loss due to fire has determined the increasing trend of forest loss in boreal forests of Eurasia during 2001-2019. (Tyukavina et l., 2022).

The following sections will describe the current situation regarding wildfires in boreal regions of Russia, the U.S., and Canada.

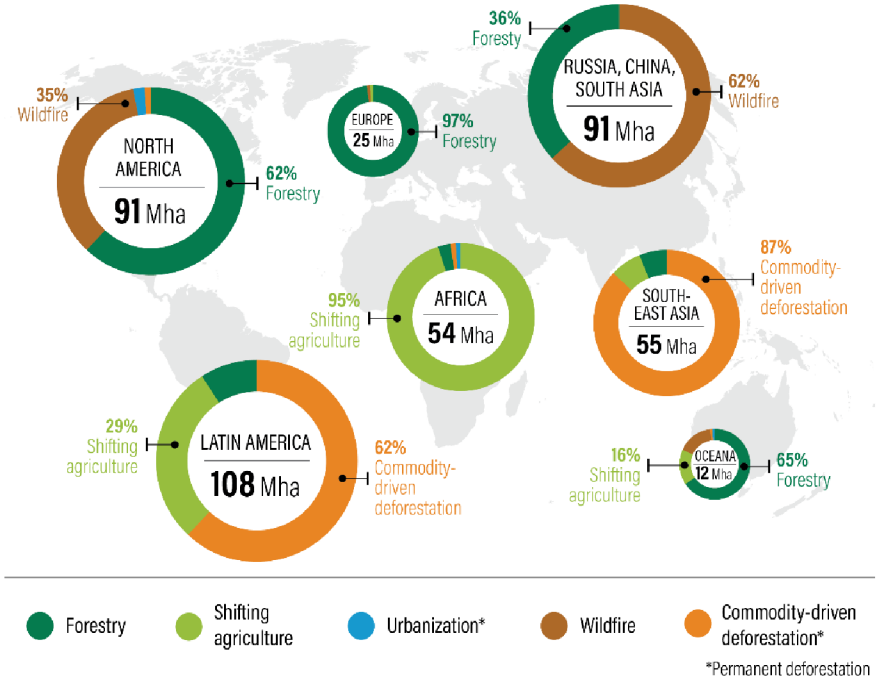

Figure 2: Drivers of tree cover loss by region, 2001-2021. Source: Global Forest Review, 2022.

3.2.1 Siberia

Siberian boreal forests represent 60% of all the boreal forests in the northern hemisphere. This number accounts for 20% of all the forests on Earth (Zyryanova et al., 2008). Russia is an absolute leader regarding the burned area of boreal forests (Tyukavina et al., 2022). Boreal wildfires in the central and eastern parts of the Siberian region usually occur in the summer and reach a maximum between June and July. However, fires in southeastern Siberia usually reach their maximum in the spring (J.-S. Kim et al., 2020). Despite the fact that the Eastern part of Siberia has a relatively short warm period, it is frequently affected by large fires. The region experienced the most severe wildfires in 2021. There were recorded around 150 thousand hotspots. The main features that contributed to the 2021 fire season were anomalous high air temperatures and anomalous drought. In total, around 9.4 million ha were burned during the fire season. The smoke plumes expanded over great distances, even up to 7 000 km. (Tomshin & Solovyev, 2022)

3.2.2 The United States

It is considered that 80% of the boreal forests of North America are intact, and approximately 13% of the area is formally protected. The boreal forest biome occupies 0.74 million km2 in the United States – mainly in Alaska state. 75% of boreal forests are managed by either the federal, state or local governments; the rest of the forests are managed by native corporations and private landowners. The timber harvest in this region is limited – less than 5% of timber harvested in Alaska originates from boreal forests. (Wells et al., 2020)

As for any other boreal forests wildfires are a part of natural processes. According to the U.S. Department of Agriculture, wildfires are now more severe and leave larger burned areas than the historical wildfire regimes. (USDA, 2021). Over the past 70 years, the burned area trend in Alaska is showing a continuous increase. The main source of the ignition is lightning strikes (Kasischke et al., 2010). It is predicted that by 2050 the burned area will increase by 24%. The main climate-related contributing factors that change the wildfire patterns include increased day and night temperatures, drought, and shortened snow season. The largest wildfires in Alaska recordedr in the past 20 years were wildfires in 2004 (Taylor Complex), in 2007 (Anaktuvuk River Fire), and in 2019 (Swan Lake) (USDA, 2021). It was determined that 360 000 ha were burned during the Swan Lake Fire in 2019. The ignition was started by a lightning strike in early July, and the consequent wildfires have lasted for several months. These severe fires were supported by perfect climate conditions: anomalous

heat waves during spring caused the early beginning of summer that continued with hot and dry conditions. (Yu et al., 2021)

3.2.3 Canada

Approximately 30% of the world's boreal forests are located in the territory of Canada. Canadian boreal forests cover about 340 million ha – that represents about 54% of Canada's forestland. Boreal forests provide important economic and social services for Canadian society. The forest sector accounted for 23.7 billion dollars in contribution to the Canadian economy in 2011 and significantly influenced rural communities' economic growth. (McGee et al., 2015)

Annually between 5 000 and 12 000 forest fires occur in Canada (Amiro et al., 2001). The highest number of wildfires take place in boreal forests. It was estimated that between 1959 and 2007 burned areas of boreal forests shared 92% of the total burned area. At the same time, only 3% of wildfires cause the most significant impact and are responsible for 97% of the burned areas (McGee et al., 2015). The average burned area usually covers 1-3 million ha, with some extreme exceptions up to 7 million ha (Aftergood & Flannigan, 2022; Amiro et al., 2001). The pattern of wildfire seasons in Canada is changing. Since the 1970s the number of wildfire events has decreased. However, the average annual burned area has doubled (Amiro et al., 2001). The shift in the patterns also resulted in the doubled frequency of large (≥200 ha) wildfire events (Schroeder et al., 2011). Several extreme wildfire events occurred in Canada during the past decade. The six most impactful wildfires during the last decade took place in western Canada. Alongside the increased severe wildfires, fire suppression costs are also constantly increasing. This increase was not predicted. The suppression costs have amounted to an average of $1 billion per year since 2014. For example, one of the costliest damages was caused by the Horse River fires in 2016. The costs were estimated at 9 billion dollars. (Hoffman et al., 2022)

The origins of wildfires in Canada at the national level are almost equally divided between natural and anthropogenic causes (Coogan et al., 2022). At the same time, at the regional level, the causes may vary. For example, lightning ignition accounts for 86% of wildfires in the Northwest Territories, whereas in Nova Scotia only 3% of wildfires were caused by lightning strikes. (McGee et al., 2015)

During the last decade, the most extreme wildfires in British Columbia burned around 1 million ha in the years 2017, 2018, and 2021. Operational costs for each of these years amounted to around $600 million (Aftergood & Flannigan, 2022). The fire season

started a month earlier than the average predictions. The region has also experienced three days of extreme temperatures rising to 50 ◦C. In total, almost 1 million ha was burned during the 2021 wildfire season. Moreover, the suppression costs were the most expensive (800 million dollars) than of any British Columbia wildfire season. (Hoffman et al., 2022)

3.3 Boreal forests and ecosystem services they provide.

A boreal forest biome or taiga (Figure 3) accounts for approximately 30% of the global forest area. This biome contains the most freshwater on the surface and contains large areas of unmanaged forests. Boreal forests occupy the northern part of the northern hemisphere mainly present in high-latitude regions of Russia, Canada, and the U.S. (Alaska). (Gauthier et al., 2015)

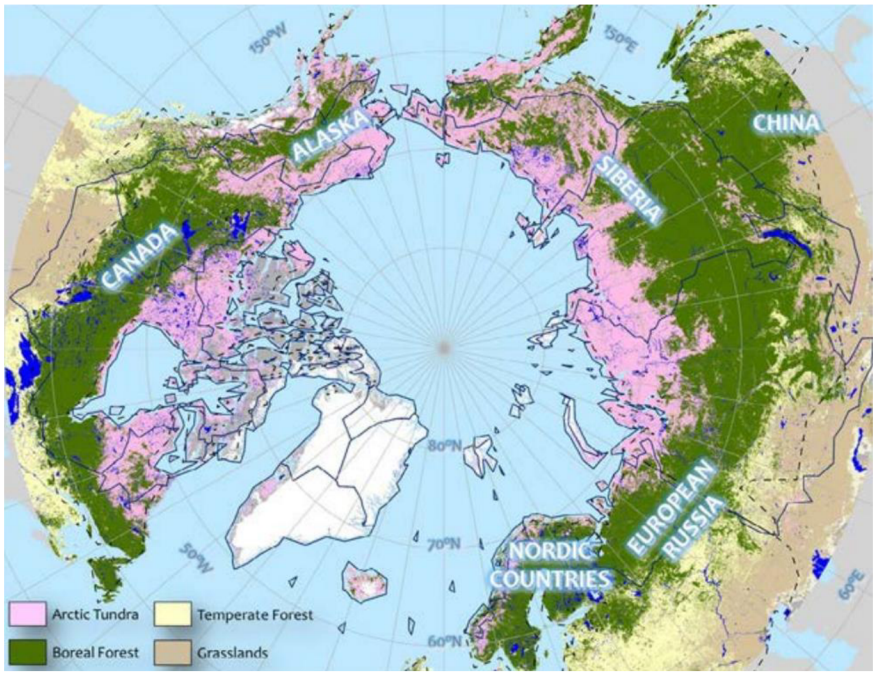

Figure 3: The distribution of boreal forest biome. Source: Hayes et al., 2022.

3.3.1 Major attributes

A strong seasonal variation is a main attribute of the biome's climate. Moderately warm and moist weather during short summers is replaced by extremely cold and dry conditions during the long winter. In the continental parts of the region (Alaska and eastern Siberia), a range in seasonal temperature extremes can reach 100°C. Annual precipitation is low throughout the boreal forest with the highest occurrence during the summer (Bonan & Shugart, 1989a).

The boreal forest is predominantly occupied by coniferous trees and characterized by low herbs or mossy floors. The species composition of forest changes throughout the region and it depends on the climatic conditions, fire regime, the occurrence of permafrost, and the disposition of water (Rowei & Scotter, 1973; Bonan & Shugart, 1989). However, the most common coniferous species belong to the following genus: Larix, Pinus, Picea, and Abies, as well as deciduous tree species from genus Betula and Populus (Tchebakova et al., 2009). When it comes to regional differences Eurasian region is mostly dominated by Larix and Pinus, and the North American by Picea genus (de Groot et al., 2013). Due to the climatic conditions, the growing season in the boreal forests is relatively short and the frost-free period lasts less than 90 days. Nevertheless, in regions above the Arctic Circle, the periods of daylight are extremely long therefore air temperature can be high during the peak of the growing season. This results in equally high daily net primary production that is present in temperate and tropical regions (Kasischke, 2000)

The boreal forests with lower annual air temperatures are also characterized by the occurrence of frozen soil or permafrost. Permafrost is also one of the determining factors that control the composition and distribution of forests. (Tchebakova et al., 2009) The presence of permafrost throughout the biome can be continuous when it is found everywhere, and discontinuous, when it occurs erratically. Permafrost in the boreal forests is primarily related to reduced decomposition rates, restrained drainage of water from the surface, and restricted nutrient cycling. Undecomposed organic soils can be found throughout the boreal ecosystems. (Bonan & Shugart, 1989; Kasischke, 2000).

Biome	Area ($\times 10^6$ ha)	Plant biomass carbon[a] (Pg = 10^{15} g)	Soil carbon[b] (Pg)
Boreal forest[c,d]	1,249	78	227
Peatlands[e]	260	<<1	397
Tundra[c]	890	<<1	180
Total	2,399	78	804

Figure 4: A summary of Carbon Present in Boreal Ecosystems. Source: Kasischke, 2000.

3.3.2 Ecosystem and social services

Being one of the largest biomes boreal forests provide ecosystem services that are beneficial for society both on a local and global scale. At the local scale, boreal forests provide such countries as Canada, Russia, and Finland with wood material for the forest industries. More than 1/3 of the lumber and ¼ of the paper have their origins in boreal regions. Local communities benefit from the boreal forests with leisure, fishing,

economic opportunities, and spiritual activities. At the global scale, the boreal region contributes to climate regulation and also represents a large reservoir of biogenic carbon. (Gauthier et al., 2015)

3.3.3 Fire regime. Resilience

Wildfires play a major role in the formation of mosaic nature, floristic composition, and diversity in boreal forests (Bonan & Shugart, 1989b). The mosaic of tree stands of different ages is a result of the last fire. In North America, large fires represent less than 5% of all fires but are related to 85% of the burned area. The rare events of severe wildfires thus determine the landscape of boreal forests rather than frequent small wildfires. (Macias Fauria & Johnson, 2008)

A crown fire (a fire that arises from the ground into the canopy) is the dominant type of fire behavior that occurs in boreal forests. Generally, fuel moisture is considered the primary determinant of fire behavior. The main reason is that the wildfires are spread by fine fuels (for example dry deadwood) that are relatively common in closed-canopy boreal forests. (Macias Fauria & Johnson, 2008)

Fire affects the temperature and moisture of soil, accumulation of organic matter, nutrient cycling, energy flow, regeneration, and productivity of the forest. In North American boreal forests, the natural fire cycle ranges from 50 to 200 years on average. Moisture balance is the main component that determines the fire cycle of the region (Bonan & Shugart, 1989a). Tree species and understory vegetation have a developed fire adaption and during dry periods are ready to ignite and burn. The intensity of the fire is primarily affected by three factors: fuel loading, fuel arrangement, and fuel moisture content. There are two types of forest fuel, living and dead, and both differ in their moisture regimes. Dead material retained in the forests with closed crowns provides highly flammable fuel. The most common source of fires in the boreal forest is lightning strikes. (Kasischke, 2000; Rowei & Scotter, 1973).

The effects of fire on site are a result of fire severity. Direct soil heating is minimal during the fire and, therefore, an effect on soil temperature is low. At the same time, the ground surface energy exchange process is greatly altered by fire aftereffects: the thickness of the insulating forest floor is reduced, the forest floor is blacked, and the forest canopy is removed. Thinning of the forest floor thickness results in reducing its insulative effect and allows greater heat flow. Hence, the soil temperature is increased and this influences the amount of removed organic matter. (Bonan & Shugart, 1989a)

A regeneration following a fire is a complex process that is hard to predict and can last many years. The post-fire vegetation depends on the type of pre-burn vegetation, the severity of the fire, the status of permafrost, topography, and the climate of the region (Bonan & Shugart, 1989a). At the same time, tree species of boreal forests have developed adaptations to fire regimes over a very long time. One example of such adaptation is the development of serotinous cones in North American pines. These cones will not release their seeds unless they are not triggered by heat (de Groot et al., 2013). Therefore, the regeneration of forest greatly depends as well on the availability of reproduction sources that consist of highly dispersed propagules, serotinous cones, fire tolerance, and vegetative reproduction (Bonan & Shugart, 1989a).

3.4 Climate change and wildfires

The climate change phenomenon is defined as long-term shifts in temperatures and weather patterns. The causes of the change can be natural or anthropogenic. The natural-caused climate change is mainly related to the variations in Earth's orbit. These variations change the amount of solar energy that reaches the planet. Due to these variations, there were eight cycles of ice ages and warm periods during the last 800 000 years. These cycles are also referred to as Milankovitch cycles – named by scientists who linked ice ages to Earth's orbital movements (NASA, 2021). However, the current climate change cannot be explained by the Milankovitch cycles. The direct driver of change is the increased amount of greenhouses in the atmosphere. It was already discovered that since the middle of the 20th century, human activities have contributed to the expansion of the "greenhouse effect." This effect explains how Earth's atmosphere absorbs energy coming from Sun and prevents the complete radiation of heat to space. The Intergovernmental Panel on Climate Change (IPCC) has composed an assessment report that highlights the increasing amount of carbon dioxide, methane, and nitrous oxide in the atmosphere is the indisputable direct result of human activities. Hence, this human impact is the main driver of changes appearing throughout the Earth's systems. (NASA, 2021.)

It is expected that the northern hemisphere will suffer the highest increases in air temperature (Macias Fauria & Johnson, 2008). The health of boreal forests is being under the pressure due to the current development and extraction of natural resources. Boreal forests have been experiencing an increase in the mean annual temperature of 1.5 °C. It is expected that the boreal forest biome will suffer the highest increase in temperatures during the next 80 years. The future warming for the boreal region may increase between 4°C and 11°C by the end of the 21st century. These kinds of changes

will probably overwhelm the resilience of ecosystems and threaten species diversity. For instance, the increased air temperature may increase the probability of wildfires and lengthens the wildfire season. (Gauthier et al., 2015).

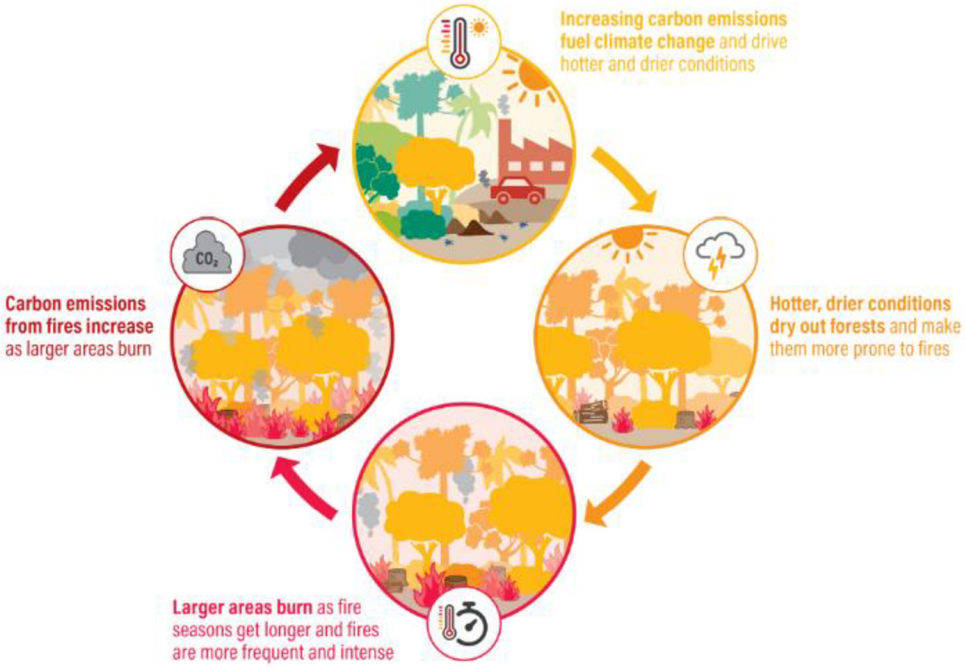

Figure 5: Fires and climate feedback loop. Source: MacCarthy et al., 2022.

Wildfires occurring in the boreal forest contribute to the release of large amounts of carbon into the atmosphere. The primary source of carbon is related to the combustion of soil's organic matter. At the same time, a part of the soil organic matter is not burned. The saved amount of organic matter is then accumulated in forests after each fire leading to a net accumulation of carbon. However, a warmer and drier climate increases the frequency and occurrence of more severe wildfires. This may provoke a shift in the carbon balance of the boreal region to the net loss of carbon (Walker et al., 2019). Wildfires are a great source of carbon and nitrogen release that will subsequently result in increased concentrations of greenhouses in the atmosphere. This may initiate a positive feedback loop between climate warming and permafrost degradation (Li et al., 2021 and J.-S. Kim et al., 2020). For example, a study conducted in the Eastern part of Siberia has determined that the rate of permafrost degradation has doubled in comparison to the degradation rate in 1975 (Badmaev et al., 2019). At the same time, the melting of permafrost will provoke a reshaping of vegetation and species composition. In the predicted warming of the Siberian climate, the area of the boreal forest is expected to reduce by 50% of the current area and will be probably substituted by steppe vegetation in 2090. (Tchebakova et al., 2009)

A restoration of post-fire vegetation depends on the fire intensity. Tree communities of boreal forests, mostly composed of conifers, are more resilient and stable. Vegetation usually quickly recovers after a light fire. However, it may be difficult to recover to pre-fire conditions after a severe wildfire. That is because severe fires limit the seed dispersal that is mostly stored in the topsoil. This represents a threat of the expansion of shrubs and broadleaf trees. (Li et al., 2021)

More severe and frequent wildfires in boreal forests provoke the increase of smoke from wildfires. (USDA, 2021). For example, during the 2019 wildfires in Alaska, smoke plumes degraded air quality over most of the state (Yu et al., 2021). Smoke from wildfires represents a threat to public health since its small particles are able to enter the lungs, as well as limit visibility and, therefore create a threat to air and ground means of transportation. (USDA, 2021)

3.5 Studying wildfires

Scientific research in the field of wildfires is gaining more attention in conjunction with the increased frequency of extreme wildfire events during the last few years. More than 13 000 scientific papers have been already published as of the beginning of 2021. Every year appear around 1 200 new articles. The papers on the wildfire domain are multidisciplinary but can be distinguished into five major divisions:

i) forest ecology and climate,
ii) detection and mapping of fire,
iii) mitigation and planning,
iv) water and soil ecology,
v) atmospheric science.

Other trends in the field also include the sub-topics such as the relationship between fire activity and climate change, fire risk modeling, and human health (Haghani et al., 2022). At the same time, research and observations on the relationships between wildfire activities and changing climate are still insufficient for the evaluation of a systematic impact (Li et al., 2021). Studying and understanding wildfires is crucial for better prediction of future fires, as well as for mitigating the impact and risks from fires on the ecological, economical, and social spheres.

Researchers use different methodologies while studying wildfires. One of these methodologies is point pattern analysis. The main goal of this analysis is to describe and explain the distribution of the events, here wildfires (Krivoruchko, 2011).

An interest in applying point pattern analysis for wildfire studying has been increasing. The points of a spatial pattern will stochastically depend upon each other. The dependence between points may be utterly complex since each point must be taken in relation to the other point. The exceptions to this dependence are the Poisson models. This model is also known as a model of complete spatial randomness or CSR. Usually, it is obvious that CSR is not realistic in the context of wildfires. It is more curious, therefore, to detect the trends in the intensity of wildfire locations and to determine whether and to what extent these trends are influenced by factors. Such factors usually consist of vegetation type, topographic characteristics of the land (slope, elevation), proximity to infrastructure or to areas inhabited by humans. (Turner, 2009)

The following sections will include a review of papers that applied methods of point patterns to analyze wildfire events. These papers consist of general quantification of wildfire patterns as of more advanced models that can be used in the context of wildfires.

3.5.1 A general spatial pattern analysis of fire events distribution

Detection of the spatial pattern is a major aspect of fire events analysis. Exemplary research that applied spatial point patterns was developed by Vadrevu and Badarinath. The authors analyzed an aggregated dataset of the 9-year count of wildfire events in Central India. This study basically explored different point pattern techniques that can quantify spatial patterns of wildfire events. To test the hypothesis of CSR the author decided to use the index of dispersion, Green's index, and nearest neighbor statistics. Ripley's K-function was also used to quantify the clustering of fires. Kernel density estimation was used for purpose of visualization of wildfire distribution (Figure 6). The authors suggested that this technique can be potentially used for the prediction of fire events. (Vadrevu & Badarinath, 2009)

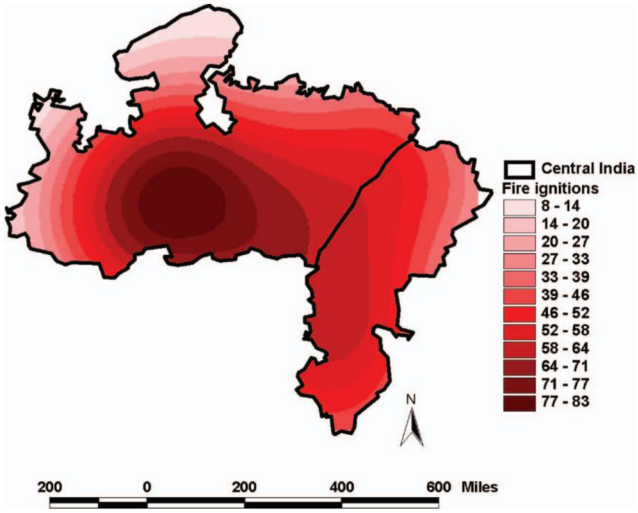

Figure 6: Kernel density estimations indicating wildfire probability in the study area. Source: Vadrevu & Badarinath, 2009.

The output from the K-function implied that the fire events tend to cluster at a lag distance of ~ 97 kilometers radius. The output map of kernel density demonstrates clear patterns of wildfire probability in the study area. Although, this research did not consider the effect of external factors on wildfire distribution. The authors conclude that the identifying pattern of wildfires is a first step that will be useful for further analysis since the resulted clustered pattern of fires might be influenced by anthropogenic or biophysical factors. (Vadrevu & Badarinath, 2009)

3.5.2 Wildfire spatial variation and external factors

Another research from the wildfire problematics sphere was conducted in the Spanish province of Castellón. The Mediterranean region of Europe has been reporting an increase in wildfire frequency during the last decades. Increment in mean temperature, decrease in relative humidity, and a rising number of abandoned farms, which provoke an accumulation of forest fuel, do not completely explain the increase in number of wildfires in the region. (Aragó et al., 2016)

An accurate prediction of future wildfires is not possible since there are many factors that influence the process of wildfire incidence. At the same time, it is possible to develop a risk map that will show the probability of ignition. Such risk maps are essential for the development of fire risk management and fire suppression strategies. The objectives of this research were to construct risk maps of the region and to identify risk factors related to fire events that occurred from 2001 to 2006. To evaluate this risk the authors have built models that were based on point processes and included covariates

that might explain the spatial variation of fires. These covariates consisted of elevation, aspect, slope, land use, and distance to the nearest road. (Aragó et al., 2016)

In contrast to the previous article authors of this research included external factors in their models. Logistic regression is considered a common tool to assess and model wildfire probability. However, for this purpose, the authors decided to apply spatial point process models. The authors fitted non-parametric kernel estimators for each year. These non-parametric estimators are usually applied for exploratory data analysis. The tool has revealed that wildfires tend to cluster in certain areas of the region. The clustering has to be considered during fitting the point process models. At the same time, the result also suggests that the clusters may be related to the independent variables (natural or human). Authors suggest that in this situation a non-homogeneous Poisson point process might be used. Ripley's K-function was also used in the study to test the CSR. In the years where the CSR hypothesis was rejected – meaning there was clustering, the authors fitted non-homogeneous Poisson process models. These models preserve an assumption that events are independent and verify whether the pattern might be explained by the factors. The authors also applied the area-interaction models since the wildfires may provoke a start of other wildfires meaning a negative interaction between the wildfire events. The models are able to model as regular point patterns as clustered. The patterns were simulated to perform a goodness of fit for both models. (Aragó et al., 2016)

The kernel estimators showed that there are hot spots in wildfire distribution within the region. At distance less than 400 m from the nearest road were recorded most of the wildfires. This factor had a neutral to negative effect on the probability of fire. Figure 7 shows the intensity function estimates for nature-caused and human-caused wildfires for the year 2006. The authors' approach to modeling fire risks can be contributed to future fire management planning since the maps show and distinguish the causes of the high fire-risk forest areas. (Aragó et al., 2016)

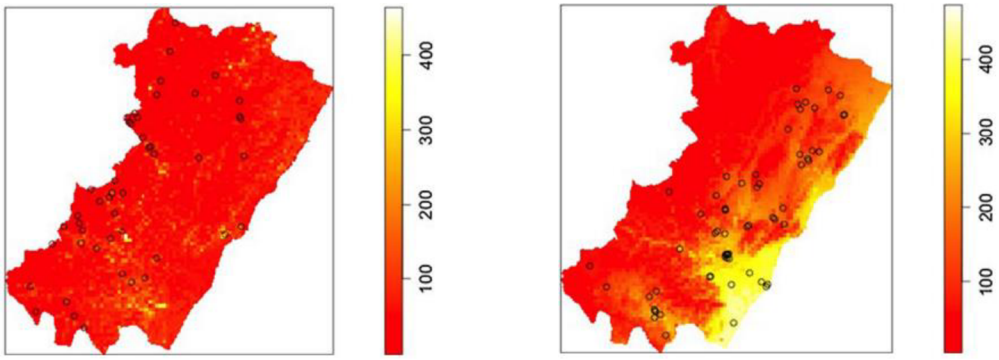

Figure 7: Estimated intensity for the year 2006 (left - natural causes; right – human causes). Source: Aragó et al., 2016.

3.5.3 Identifying and analyzing spatial and temporal patterns of wildfires

Another example of point pattern analysis used in modeling wildfire distribution was developed by Aftergood and Flannigan. The study conducted in Western Canada tested temporal- and spatial-distribution variability of lightning-ignited wildfires that occurred from 1981 to 2018. Several studies recorded the clustering tendency of lightning-originated wildfires on the landscape. The impacts of climate change on lightning have been concerning researchers since the end of the last century. Storm activity and lightning frequencies were predicted to increase in Northern America by the middle of the 21st century. As climate change violates ecosystem dynamics it also can challenge ecological communities and urban areas with more frequent and severe wildfires. The study conducted by Aftergood and Flannigan aimed to examine patterns of wildfire events and trends related to such patterns. (Aftergood & Flannigan, 2022)

The study area located in ~4.4 thousand km2 area consisted of forests in the province of British Columbia, Canada. The authors considered only lightning-ignited wildfires that occurred between 1981 and 2018. To address the questions authors applied the point pattern process. To detect deviations from CSR at different distances authors applied a well-known K-function. Due to the non-parametric characteristics of the dataset, a non-homogeneous K-function was used. The Getis-Ord Gi* statistics were applied to identify hot spots (significant clustering) and cold spots (dispersal) within the wildfire pattern. Aftergood and Flannigan also tested a correlation between the time sequence and the rank observations. For this purpose, the Mann-Kendall statistics were computed for the wildfires events that occurred during the whole 38-years period. (Aftergood & Flannigan, 2022)

The result from K-function demonstrated a deviation from the CSR null hypothesis meaning the presence of clustering in each studied year. The output from the Getis-Ord Gi* has demonstrated the significant spatial and temporal clustering of wildfires. However, the clustering between months slightly differs. Significant clustering occurred only in the central part of the study area in June, however, in August the clustering was observed in the southeastern part of the study area. (Aftergood & Flannigan, 2022)

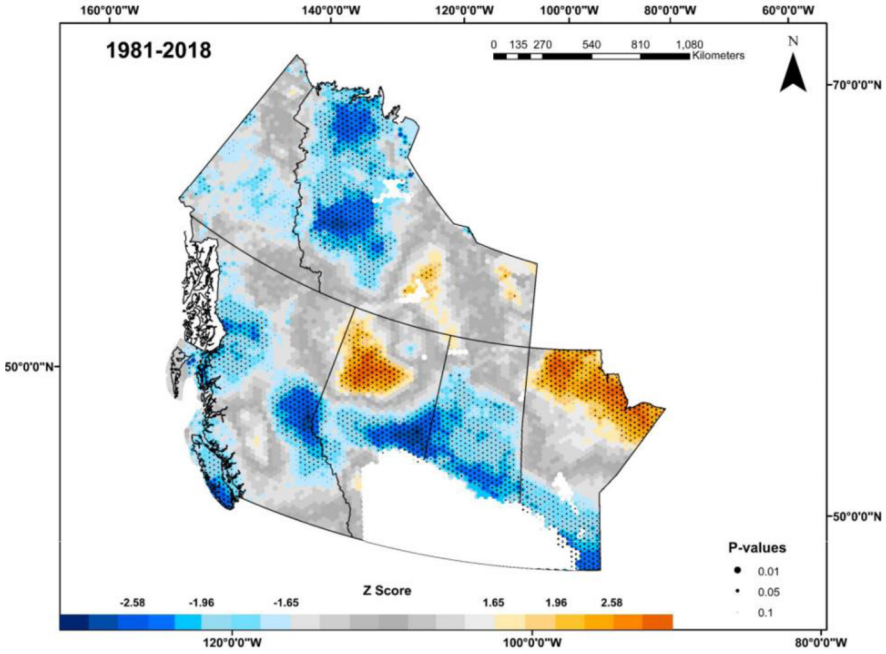

Figure 8: Mann-Kendall trend statistics: orange – increasing trend, blue – decreasing trend. Source: Aftergood & Flannigan, 2022.

The Mann-Kendall model has detected temporal trends in the number of fires. While some regions showed a decreasing trend in wildfire number events (central-eastern British Columbia, Saskatchewan), other regions demonstrated increasing trends (northwestern areas of Alberta, northeastern and central British Columbia). (Aftergood & Flannigan, 2022)

3.6 Wildfire management

3.6.1 Canada

Research from Tymstra et al. distinguishes six phases of wildfire management in Canada (Figure 9). These phases include prevention, mitigation, preparedness, response, recovery, and review. The prevention phase is aimed at preventing wildfires; the mitigation phase is focused on reducing the impacts of the wildfires; the preparedness phase includes actions that ensure the readiness to manage the arrivals of wildfire and their aftereffects; the response phase incorporates actions that have to be taken when a wildfire emerge, the phase of recovery is aimed at restoration of conditions impacted by wildfire. The authors also distinguish a review phase among the wildfire management phases due to the fact that wildfire management in Canada evolves and upgrades based on the implementation of recommendations concluded from the post-wildfire seasons and reviews. (Tymstra et al., 2020)

Figure 9: The six phases of wildfire management. Source: Tymstra et al., 2020.

Since Canada is a confederation containing ten provinces, governments in Canada have adopted an all-hazard approach to managing such disasters as wildfires effectively. The federal government is responsible for emergency management at the national level, with about 10 % of emergencies requiring engagement from the federal government – usually when a province is not able to cope with the emergency. Moreover, the federal government can engage in management when a wildfire has national aftermaths. Several governmental bodies have fire control agreements with each other to ensure that services are ready to respond to the wildfire and to share management and responsibilities of wildfires within their bodies. (Tymstra et al., 2020)

The entire territory of British Columbia lies within the full wildfire suppression management zone. The Province of British Columbia highlights the following response priorities in their policies:

1. Human life and safety
2. Other priorities:
    - 2.1 infrastructure, communities, other assets;
    - 2.2 mitigation of impacts on key environmental values;
    - 2.3 maintenance of other natural resource values

The provincial strategy of British Columbia prescribes a response to each wildfire incident. At the same time, this strategy considers a mild reaction to the wildfires, such

as monitoring and managing those wildfires that represent a minimal risk to the priorities mentioned in 2.1. from the list of response priorities (Tymstra et al., 2020). The British Columbia Wildfire Service (BCWS) is responsible for wildfire management activities within the province. According to the B.C. Wildland Fire Management Strategy, when the BCWS receives a notification of a wildfire – most wildfires are reported by the public or during aerial patrols, the initial attack of a three-person crew is assigned to the declared area. In terms of when a wildfire cannot be managed during the initial phase, another team of twenty persons and heavy equipment are dispatched to the site. Suppose there is a deficiency in staff and equipment resources. In that case, the responsible body can request help from other Canadian provinces or abroad (based on resource-sharing agreements). The variability in wildfire size, the complexity of wildfire suppression, and the volume of used resources result in higher variability in wildfire suppression expenditures. (MacMillan et al., 2022)

The British Columbia consists of six regional fire centers that have a responsibility for wildfire management within the designated zones. The fire centers of the province can be observed in Figure 10. These fire centers are also distinguished into the local fire zones. (Province of British Columbia, 2022)

Figure 10: Regional fire centers of British Columbia. Source: Province of British Columbia, 2022.

The fire centers are coordinated by the Provincial Wildfire Coordination Centre (PWCC) in terms of such functions as aviation management, GIS, finance, administration, and resource management. (Province of British Columbia, 2022)

The Canadian Council of Forest Ministers (CCFM) issued an Action Plan for wildfire management in Canada for the years 2021 – 2026. This Action Plan describes six actions that are crucial for increasing the communities and infrastructure of Canada's resilience to wildfires by 2030. This goal is planned to achieve by means of shifting the focus of wildfire management "from forestry-centric to a whole-society perspective." (Canadian Council of Forest Ministers, 2021)

The government established the Canadian Wildland Fire Information System to monitor and daily forecasting fire weather during the wildfire season. One of the components of this system is the Forest Fire Weather Index System (FWI). The calculation of this index is based on temperature, wind speed, relative humidity, and 24-hour precipitation. These variables are consequently used to calculate the six components of the FWI. The FWI also includes elevation data for future interpolation of the weather data to produce gridded maps. (Government of Canada, n.d.)

3.6.2 Alaska

When it comes to Alaska (the U.S.) the wildfire protection strategy is prescribed by the Alaska Interagency Fire Management Plan. Four categories of protection levels are distinguished within the state (International Arctic Research Center, 2020). These categories can be observed in Figure 11. The initialization of the response on new wildfires is usually determined by the protection zone and the available resources. Management of wildfire suppression activities are divided between the Bureau of Land Management (BLM) Alaska Fire Service, the US Forest Service, and the Alaska Division of Forestry. (International Arctic Research Center, 2020)

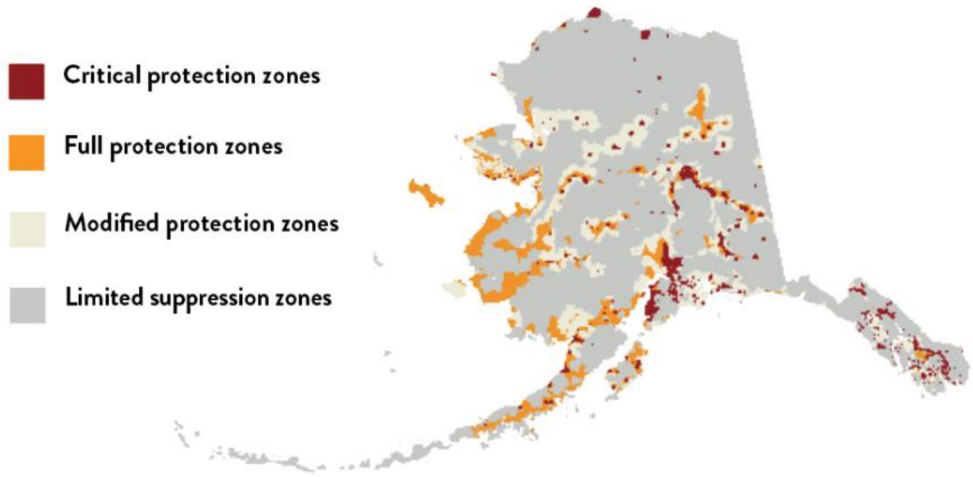

Figure 11: Categories of wildfire protection in Alaska. Source: International Arctic Research Center, 2020.

The Alaska Interagency Wildland Fire Management Plan was developed to determine what kind of management actions will be initiated regarding wildfires. These actions range from periodic observations to immediate suppression of wildfires (Alaska Wildland Fire Coordinating Group, 2015). The Federal government established the Joint Fire Science Program (JFSP) to fund research in wildfire problematics for future policy and land management implementation. This program has supported the Alaska Fire Science Consortium (AFSC), which has comprehensive researchers, practitioners, and managers in addressing problems of wildfire management. Moreover, an already-described Fire Weather Index System (FWI) from Canada is also used in Alaska for forecasting the risks of wildfires. (International Arctic Research Center, 2020)

4. Study area and methodology

4.1 2021 Wildfires in British Columbia, Canada

The province of British Columbia is located in the western part of Canada – bordering the mountain range of the Rocky Mountains on the east and the Pacific Ocean on the right. The climate is, therefore, influenced by the ocean and mountain ranges (Government of Canada, 2015). A mild climate persists during the whole year in areas along the south coast: daytime temperatures reach around 20°C in summer, and during the winter the temperature rarely drops below 0°C (Province of British Columbia, 2022)

Figure 12: Location of British Columbia. Source: own data processing, Open Street Maps.

Proximity to the ocean, change in topography, and latitude influenced the diversity of the ecosystems present in the province. Such ecosystems include boreal forests, alpine tundra, grasslands, semideserts, and temperate rainforests. Wildfire ignition and pattern depend on the characteristics of each ecosystem. These characteristics embrace such factors as fuel moisture and drying rates. High-moisture air from the Pacific Ocean is usually brought by the midlatitude storm track that, therefore, influences the moisture content of the fuel. However, during summer the high-moisture air is blocked by the North Pacific High. This leads to dry and warm conditions that influence the dryness of the fuel. It is assumed that climate change may cause the increased block of the high-moisture flow and the drought period will extend. (Coogan et al., 2022)

The official duration of wildfire season acknowledged in most western Canadian provinces is from the 1st of April to the 30th of September (Aftergood & Flannigan, 2022). The fire activity in British Columbia has seen new records in recent years. The highest amount of burned area was recorded during the 2017 and 2018 wildfire seasons (Figure 13). A 10-year average of the burned area is 348 917 ha.

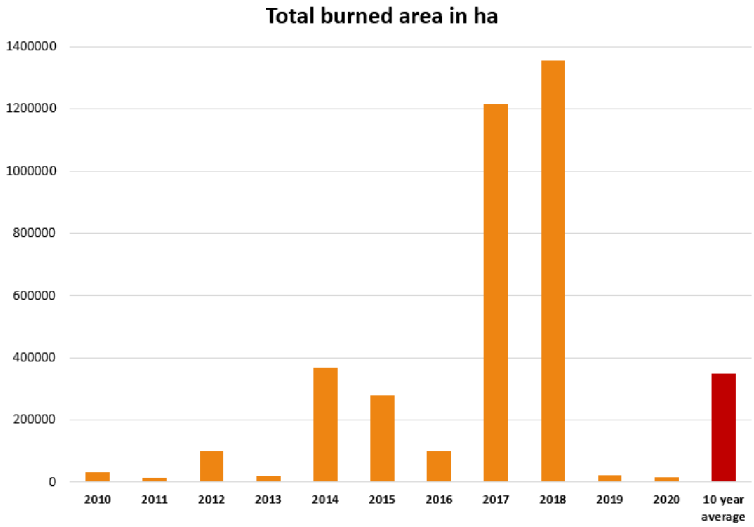

Figure 13: Statistics of total area burned during the last 10 years. Source: Province of British Columbia, 2022, own data processing.

The 2021 heat wave was one of the factors that provoked extreme wildfires (Coogan et al., 2022). It was recorded that the southern part of British Columbia received below-average precipitation during the autumn and winter. Therefore, the extended drought conditions then continued in April, May, and June. At the same time, the precipitation rate in the northern part of the province was average. Later in June, the northern part received its average rainfall rate, while in the southern part occurred only 30% of the usual rainfall in June. Along with the decreased amount of precipitation, the air temperature extremely raised. As a result, the extreme heat and atypical drought provided burning conditions that normally occur in August. These prone-to-ignition conditions remained unchanged throughout the first two weeks of July. Lightning events contributed to emerging of new wildfires. Around 40 new wildfires ignited in British Columbia every day. Moderate rainfall occurred in the province's northern regions in the second half of July. Nevertheless, the amount of felt precipitation was insufficient to suppress large wildfires. Daytime conditions persisted hot and dry in August. At the same time, the number of daylight hours was slowly decreasing, and in relation to that, cooler temperatures and higher moisture allowed overnight recoveries. In addition, varying rainfall helped to mitigate the dangers of wildfire and wildfire activities. By the

end of August, fire activity and temperature rate returned to seasonal norms. (Province of British Columbia, 2022)

Fire Centre	Number of Wildfires	Hectares Burned
Cariboo Fire Centre	270	129 537
Coastal Fire Centre	216	7 100
Kamloops Fire Centre	459	497 497
Northwest Fire Centre	58	28 645
Prince George Fire Centre	274	128 881
Southeast Fire Centre	367	77 615
Total	**1 642**	**869 279**

Table 1: Wildfire statistics by fire center – wildfire season 2021. Source: Province of British Columbia, 2022.

4.2 Data

4.2.1 Wildfire events dataset

The data represent the points of recorded wildfires in the study area during the 2021 wildfire season. The dataset was obtained in the form of kmz* format that was converted to the shapefile format from the governmental website of the province of British Columbia. The dataset consisted of 2 993 points representing the location of recorded wildfires within the period from the 1st of January 2021 to the 22nd of March 2022. Only wildfires that occurred from the 1st of April to the 30th of September will be included for the purpose of the study. Other recordings that were missing information on the date and duplicated recordings were deleted. The records lying outside the demarcated have been excluded as well. Figure 14 shows the original raw data on the left and cleaned data on the right.

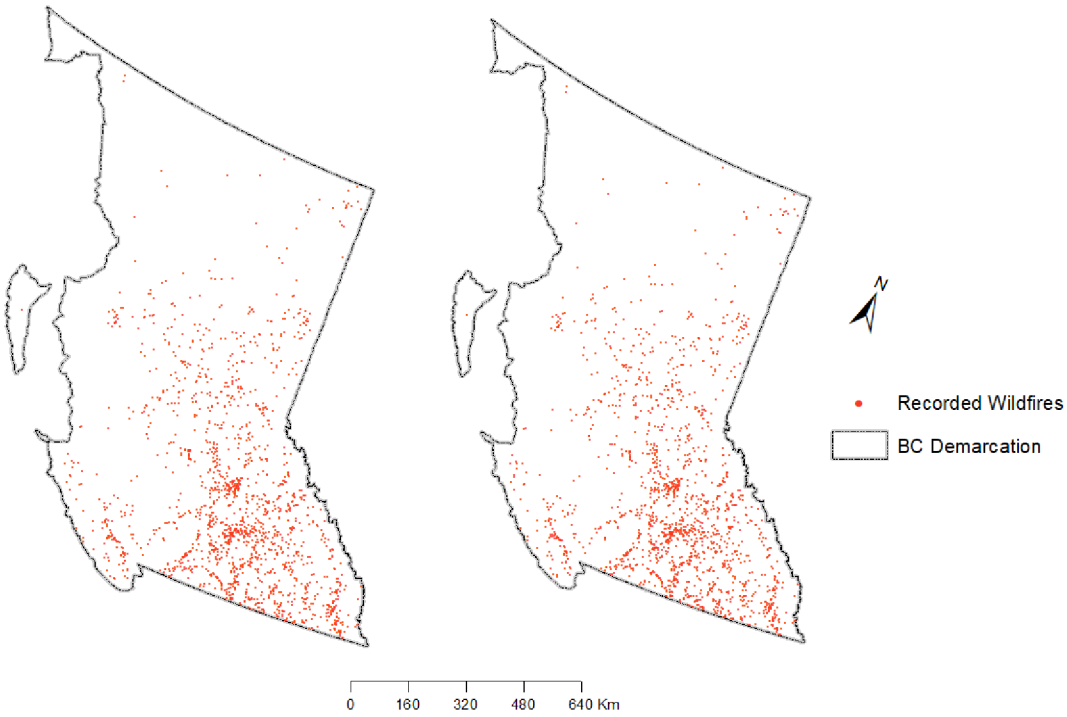

Figure 14: The location of wildfires in the study area. Raw and processed data. Source: Province of British Columbia, 2022; own data processing.

External factors will be taken into consideration to understand the pattern of the wildfire events better. These factors include vegetation zones, average fuel moisture rate, average drought rate, and proximity to the major road.

4.2.2 Contributing factors

Vegetation zones

According to Baldwin et al., five vegetation zones are distinguished within the province of British Columbia: alpine tundra, boreal forests, cordilleran forests, grasslands, and pacific cool temperate forests. Each zone is characterized by elevation, climate, and vegetation type. Alpine tundra zones occupy areas of ~ 200 000 km2, commonly near-above treeline on high elevations and mountains in central, northern, and southern parts of British Columbia and on the coast of the province. The climate is determined by low temperatures, wind, and snowfalls. Landcover represents a mosaic of low and shrub vegetation accompanied by exposed rocks. Discontinuous permafrost is present occasionally. Average annual temperatures can vary from -5°C to +1°C. The average annual precipitation usually varies between 1800 mm and 4700mm on the coast and between about 650 - 3500 in the central and southern parts of British Columbia. Boreal forests mostly occupy the northern and east-northern regions of the province. The climate is characterized by short summers and long winters. Land cover is mostly

dominated by forests. However, numerous rivers and water bodies diversify the landscape. The average annual temperature can vary from -5°C to +2°C, and average annual precipitation usually varies from 300 mm to 600mm. Cordilleran forests occupy most of the territory of the province. Due to the orographic effects of the coast and mountains, the climate here is temperate and humid. Temperatures here are more moderate than in the boreal forest zone and usually vary from 2°C to 5°C (average annual temperature). Precipitation rate is highly variable – it varies between 600 mm and 2000 mm. The southern Cordilleran forests are determined by lower precipitation (between 400 and 800 mm). The forests are usually dominated by coniferous species. Grasslands are situated at the lowest elevations and cover an area of 2 500 km2 in south-central British Columbia. The vegetation is dominated by drought-tolerant bunch grasses (Poaceae) and drought-tolerant shrubs. The climate is characterized by moderate winters and warm summers (the average annual temperature is about 8°C). Average annual precipitation is low – usually less than 380 mm. Pacific cool temperate forests are situated along the west coast of British Columbia and cover about 110 000 km2. The climate is wet and cool. The landscape is dominated by coniferous forests. The climate is characterized by moderate temperatures (average annual between 3°C and 10°C) and high precipitation rates (between 1000 and 2000 mm). (Baldwin, 2020)

The data were obtained from the website of the Government of Canada. The original dataset was subsequently converted to a raster for future calculations. Figure 15 shows how vegetation zones are distributed within the study area.

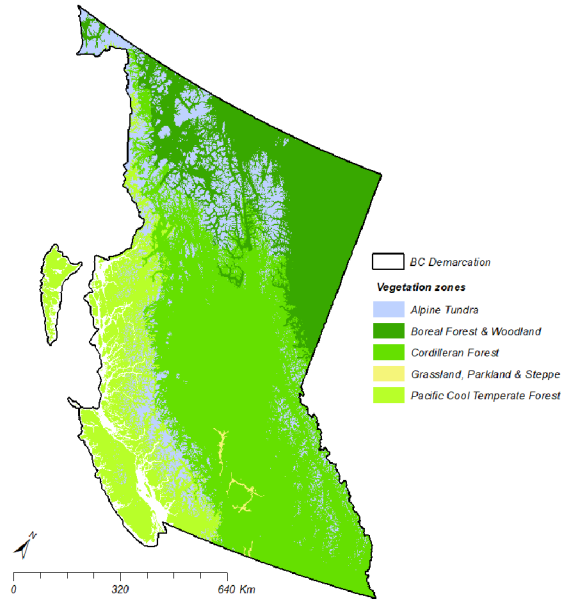

Figure 15: Vegetation zones of British Columbia. Source: Government of Canada, 2022; Baldwin et al., 2019.

Mean wind speed

Wind speed is considered to be a factor that may affect the risk of wildfires (Aragó et al., 2016). The Canadian Forest Fire Weather Index System includes wind speed for the calculation of the Initial Spread Index of wildfires. (Government of Canada, 2022)

For the purpose of the thesis, the annual mean wind speed data were included in the calculations. The dataset was obtained from the Global Winds Atlas website. The visualization of data is shown in Figure 16.

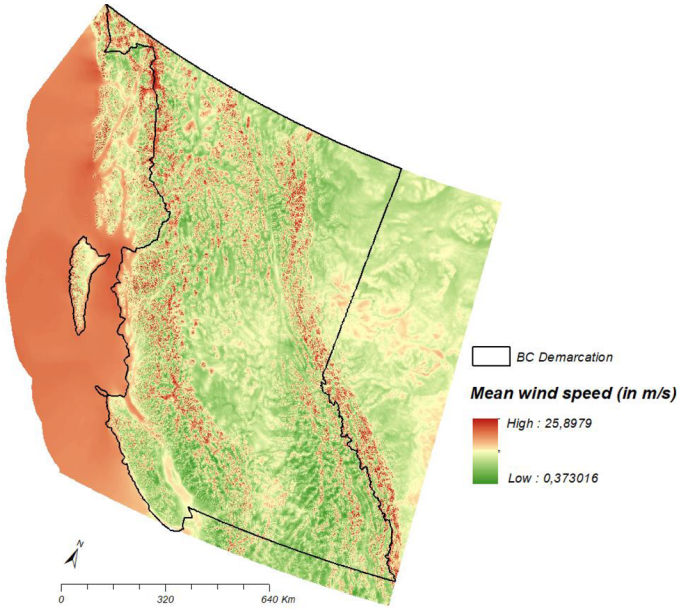

Figure 16: Annual mean wind speed throughout the British Columbia for year 2021. Source: The Global Wind Atlas 3.0, 2021, own data processing.

Major roads

Several literature sources imply that human-caused wildfires tend to cluster in proximity to population centers or components of anthropogenic activities such as roads or railroads (Coogan et al., 2022). This factor was chosen as a proxy for anthropogenic activities within the study area. The dataset was obtained from the website of the Government of Canada in ESRI shapefile format. The Euclidean distances were calculated. Subsequently, the dataset was exported as an *.img raster image. The original layer and a resulting raster are depicted in Figures 17 and 18.

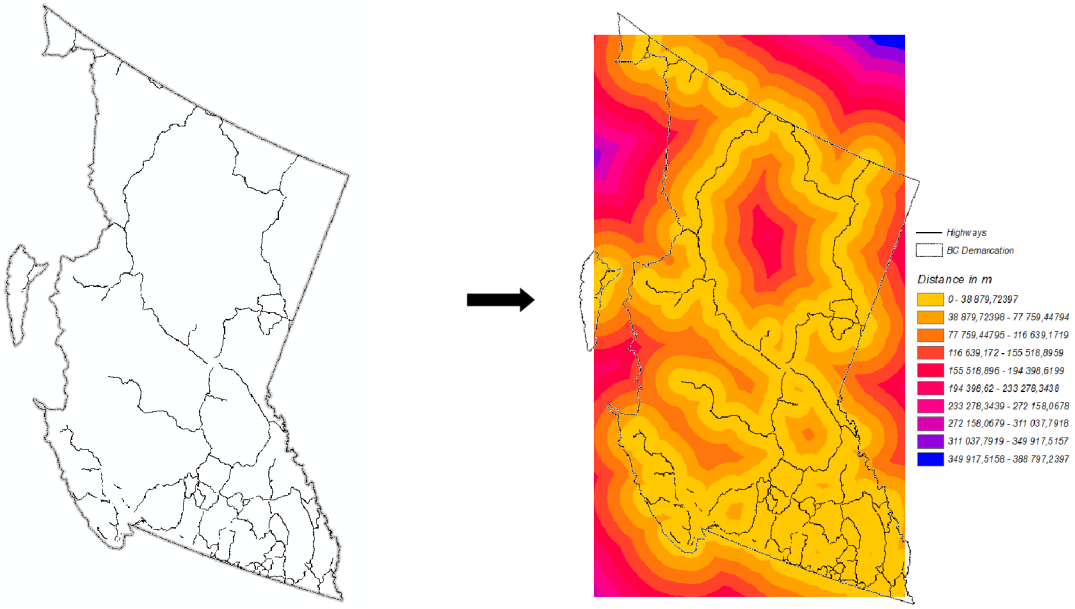

Figure 17 and 18: An original shapefile of major roads in the province of British Columbia (left); calculated Euclidean distances from the roads (right). Source of original data: Government of Canada, 2022; own data processing.

Average drought level

Drought occurs in British Columbia usually due to combinations of insufficient snow accumulation during the winter, delays in rains, or dry and hot weather. A six-level drought classification (0 – no impact at all, 5 – the highest, almost certain impact) system is used in British Columbia to assess the severity and response to drought (Province of British Columbia, 2022).

The dataset was obtained from the ArcGIS catalog in the ESRI shapefile format. The data were aggregated to represent average drought levels across the British Columbia region during the wildfire season. The processed layer of average drought levels is visualized in Figure 19.

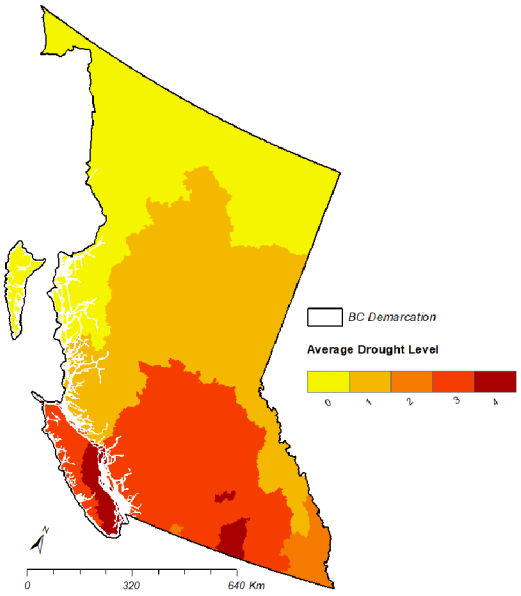

Figure 19: Average drought levels across the province for the period of 2021 wildfire season. Source: Province of British Columbia, 2022; own data processing.

4.3 Methodology

Point pattern analysis will be used to determine the pattern of wildfire events that occurred in British Columbia during the 2021 wildfire season. The concept of the 1st and the 2nd order effects is important within the point pattern analysis domain. (Gimond, 2018)

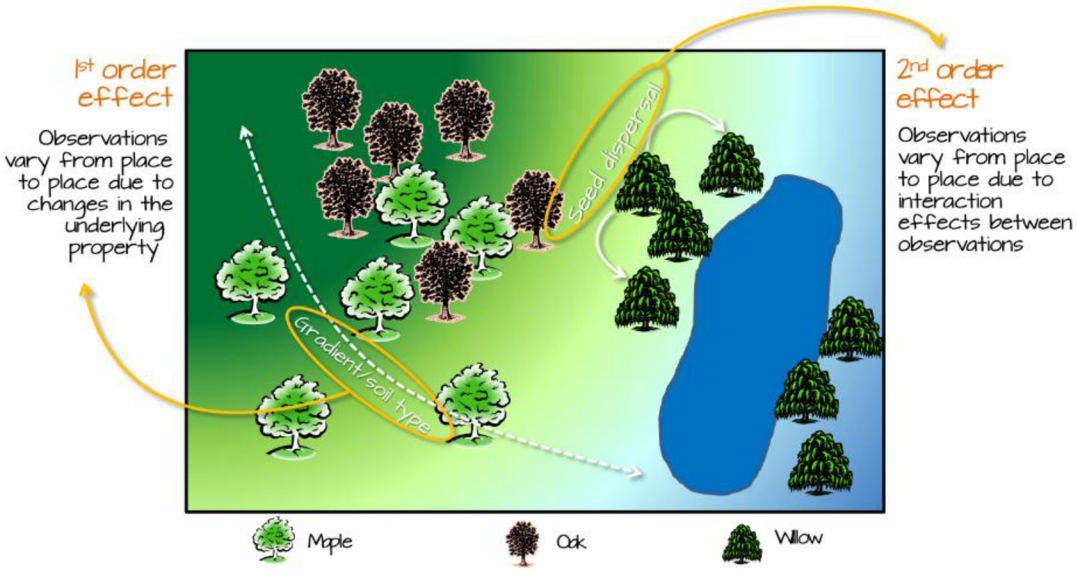

Figure 20: The 1st and 2nd order effects as an example of tree distribution. Source: Gimond, 2018.

As it is described in Figure 20 the so-called 1st order effects can be described by density methods. The patterns in terms of the 2nd order effects are described by the interaction between observations – distance. (Gimond, 2018)

4.3.1 Distribution of fires in terms of 1st order effect – the kernel density approach

The kernel density is a nonparametric method. It is used to create smooth maps of density. This method is based on counting the number of events within the overlapping sub areas. It generates a kernel - a moving subarea window. The kernel approach provides a grid of density values. Each cell of the grid will be assigned the density value computed for the kernel window centered on that cell. The weight of points can also be taken into consideration in kernel functions. The influence (weight) of the neighboring points decreases with the growing distance from their kernel center. (Grekousis, 2020)

4.3.2 Distribution of fires in terms of 2nd order effect

Ripley's K-function

Methods focused on the 2nd order effects of the process explore how the points are distributed in relation to each other. In the other words, these methods are based on distance. Two of the most common distance-based methods are the K- (L-) functions and the average nearest neighbor (Gimond, 2018). In this thesis, the K- (L-) functions will be applied.

Ripley's K-function is aimed to describe the occurrence of events throughout the whole study area. K-function tests the null hypothesis of complete spatial randomness. The principle of the K-function is calculation of the average number of points within distance divided the average number of points per unit of area. If the K values are larger than it is expected to be, it means that the points are clustering at given distance range. Smaller than the expected K values indicate a dispersed nature of points. (Krivoruchko, 2011; Gimond, 2018)

$$\widehat{K}(h) = \frac{1}{\lambda n}\sum_{i=1}^{n}\sum_{j\neq i}^{n}\frac{1}{\omega(s_i, s_j)} I(h_{ij} \leq h) \quad (1)$$

In Ripley's K-function h is a distance from an arbitrary point, λ is the intensity of the pattern, h_{ij} is distance between points i and j, I is an indicator (if $h_{ij} \leq h$ then I is 1, if $h_{ij} > h$ then I is 0), $\omega(s_i, s_j)$ is the edge correction factor, n is a number of observations (Krivoruchko, 2011). This function can be plotted for comparison with the expected K-function. (Gimond, 2018).

A drawback of the K-function is that due to the curved shape of the function, it might be difficult to recognize slight differences between the expected K and the calculated K.

Therefore, a normalized K-function was defined – an L-function. This transformation is usually used when the pattern is close to random. (Krivoruchko, 2011; Gimond, 2018).

$$\hat{L}(h) = \sqrt{\frac{\hat{K}(h)}{\pi}} - h \tag{2}$$

A major advantage of the K-function is the ability to measure point pattern distribution along the scale. This capability is very important for the reason that many spatial process characteristics tend to change within the scale. (Krivoruchko, 2011).

G-Function

The distance-based G-Function is used to describe variations of point patterns. It calculates the cumulative frequency distribution of the nearest neighbor distance of a point pattern and can be written as:

$$G(d) = \frac{\mathrm{sum}(D_{ij} < d)}{n} \tag{3}$$

Where $\mathrm{sum}(D_{ij} < d)$ is the number of point pairs i and j with a distance smaller than d divided by the total number of points n. The interpretation the of G-function follows that values $\hat{G}(r) > G_{pois}(r)$ suggest a clustered pattern, whereas values $\hat{G}(r) < G_{pois}(r)$ suggest a dispersed pattern. (UCGIS, 2023; Baddeley, 2010)

4.3.3 Modeling wildfire distribution

"Any kind of data analysis or data manipulation is equivalent to imposing assumptions" A. Baddeley. It would be inappropriate to posit the statistical significance of the phenomena unless the model was not assumed. Hence, the goal of statistical modeling is to make these assumptions definite. The fitted models are, therefore, useful for the summary of the data and for making predictions. Moreover, the models can be simulated – it is possible to generate a random pattern based on the model parameters. (Baddeley, 2010)

Point process models are used to model point patterns. A full explanation and formulation of point process theory lie beyond the scope of this diploma thesis. Here will be described only the theoretical parts that are relevant to the research. One

example of such a model is the uniform Poisson process. This model is often related to a model of complete spatial randomness (CSR), meaning that the points of a uniform Poisson process are randomly distributed and are independent of one another (Baddeley, 2007). The kernel density (described in section 4.3.1) can be adjusted to model the relationship between the distribution points and some covariates. This relationship can be defined mathematically using a Poisson point process model:

$$\lambda(i) = e^{\alpha+\beta Z(i)} \tag{4}$$

here $\lambda(i)$ is the modeled intensity at location (i), e^{α} is the base intensity (when the covariate is 0), e^{β} is the multiplier that determines how much the intensity increased/decreased for each 1 unit increase in $Z(i)$ (covariate). (Gimond, 2018)

There are other point process models that might be applied. For example, the Cox models and Gibbs models. These modifications of the Poisson process models allow points to depend on one another. (Brown et. al, 2021)

In case of rejected CSR and the presence of evidence for clustering, non-homogeneous Poisson process models will be applied. The resulting models will be assessed using a likelihood score - the Akaike Information Criterion (AIC). The lower AIC indicates a better fit of the model. (Baddeley, 2010)

A free and open-source RStudio software (version 2021.09.1), ESRI ArcMap software (version 10.8.2), and open-source QGIS (version 3.22.1) were used for data analysis and visualization.

5. Results

The exploration of data is an essential initial phase of any scientific method therefore, the summary statistic was calculated for the wildfire events data. The number of wildfires during the wildfire season 2021 showed high variability, with an average number of 283 wildfires per month. The higher deviation from the average was discovered in July and September. According to Table 2, the highest number of wildfires occurred in July – in total, 787 wildfires. The lowest number of wildfires occurred in September – 58 wildfire events.

Month	Number of wildfires
April	171
May	127
June	279
July	787
August	278
September	58
Total	**1 700**

Table 2: Counts of wildfires by month occurred in British Columbia. Source: own data processing

A basic point pattern analysis summary statistics were calculated for the wildfire events. Figure 21 shows the location of the mean center, median center, and standard distance (a measure of the variance). The standard distance is 309 kilometers.

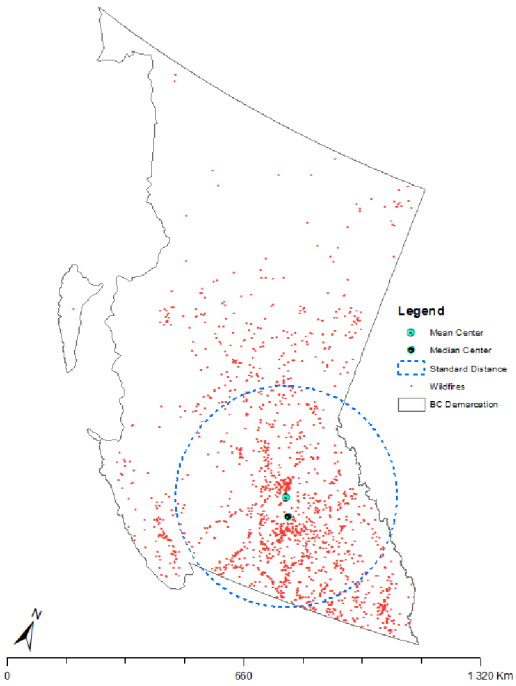

Figure 21: Summary statistic of the wildfire events. Source: own data processing.

5.1 1st order effects

The kernel density estimators were calculated for each month of the 2021 wildfire season in British Columbia. Several hotspots were indicated across the study area. The estimates are depicted in Figures 22-27. The maps for each month show that wildfires tend to occur in the southern and central parts of British Columbia, therefore, forming clusters.

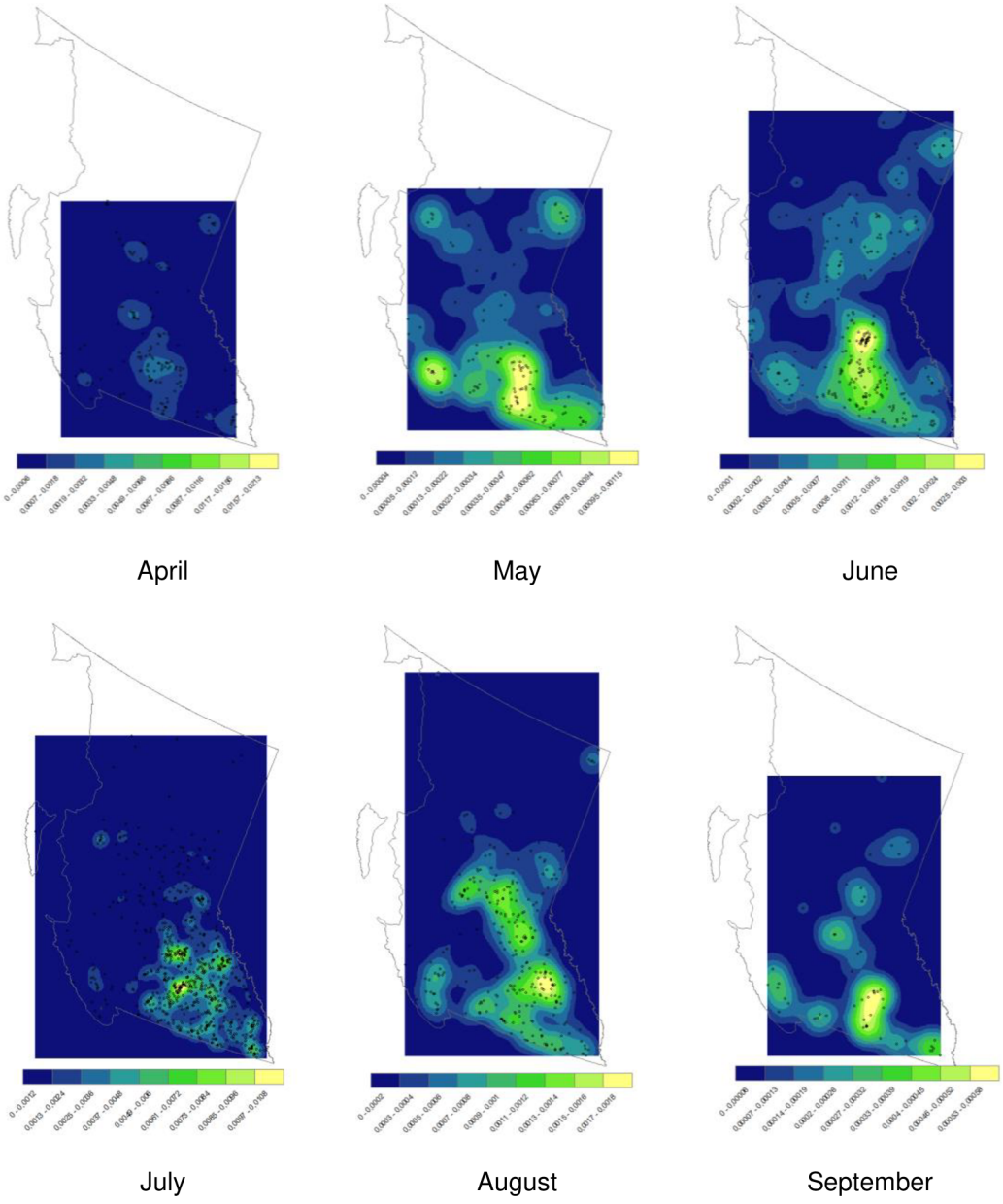

Figures 22-27: Kernel density estimators for wildfires occurred in British Columbia during 2021 wildfire season. Source: own data processing.

It can be observed that the weakest clustering appeared during April while the rest of the months showed stronger clustering. At the same time, wildfires that occurred during

May and June show a clustered pattern in different parts of the province. Clusters of July showed the lowest dispersal with the highest occurrence in the southeast. These clusters may be affected by external factors. At the same time, the resulted clustered type of point pattern suggests that clustering should be considered during fitting the model of the influence of external factors to the observed patterns.

5.2 2nd order effects

As was described in section 4.3.2 this method is focused on the 2nd order effects of the pattern – interaction between the points themselves. For this purpose, an extension of Ripley's K-function – an L-function was used to explore the 2nd order effects throughout the whole study area. A plot on Figure 28 shows an L-function applied for all the wildfires that occurred during the 2021 wildfire season.

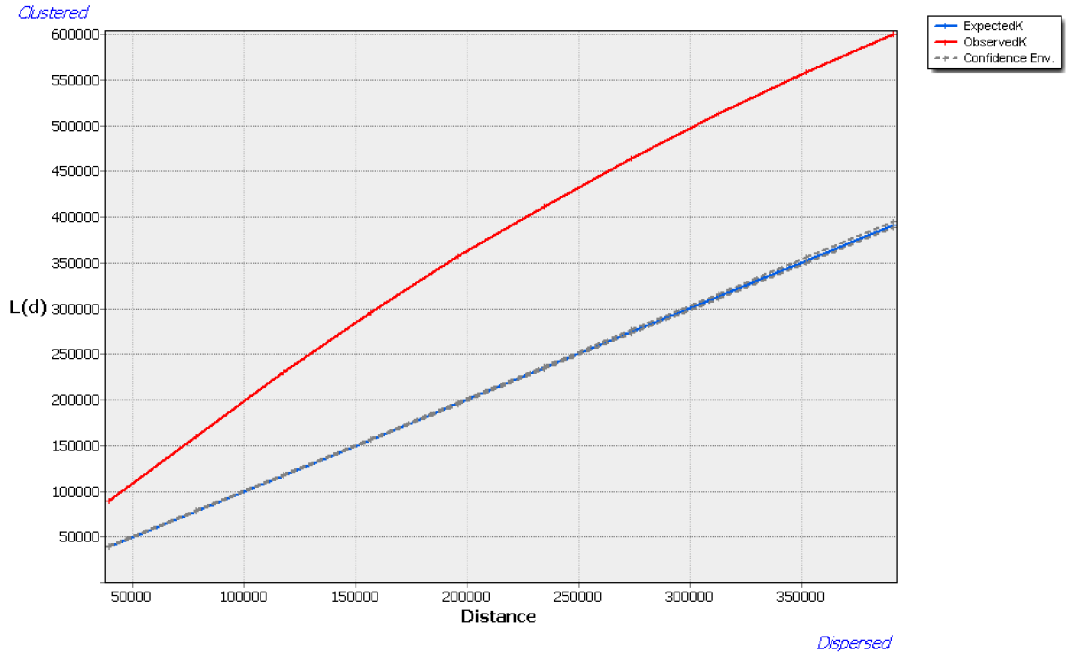

Figure 28: Estimates of L-function (whole wildfire season). Source: own data processing.

The plot suggests that the pattern of the wildfires is clustered at all distances (in m) – the observed L values are greater than the expected L values. As a result, a null model of Complete Spatial Randomness is rejected. Patterns of wildfires were explored for each month of the wildfire season separately. Figures 29 – 34 visualize the comparison of obtained L-functions for each month.

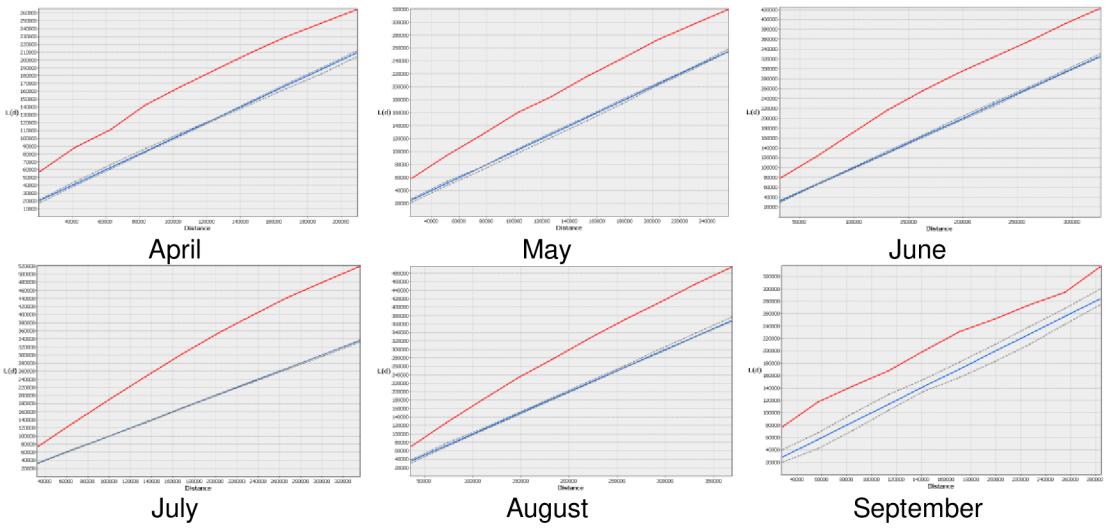

Figures 29 – 34: L-function for each month. Source: own data processing.

It is obvious from the plots that the observed K value is greater than the expected K value. Moreover, the observed K values fall outside of the confidence envelope range. Therefore, the pattern of wildfires is considered significantly clustered at all distances in each study month.

In addition to the L-function a G-function was used to investigate 2nd order interactions between wildfires and external factors. Plots on Figures 35 – 39 show the interaction between wildfires and vegetation zones. It is visible that the values of $\hat{G}(r)$ are smaller than $G_{pois}(r)$ for all of the vegetation zones except for Alpine Tundra. This result indicates that the nearest neighbor distances in the point pattern are shorter in comparison to a Poisson process. This result, therefore, indicates a correlation between the factor and wildfires.

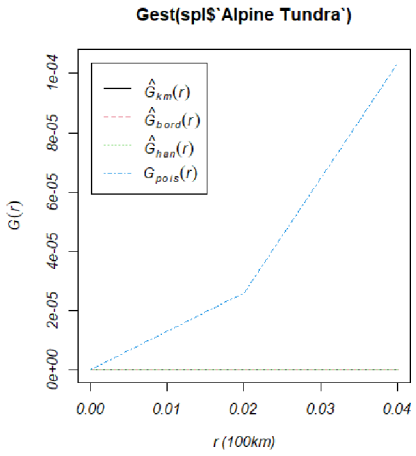

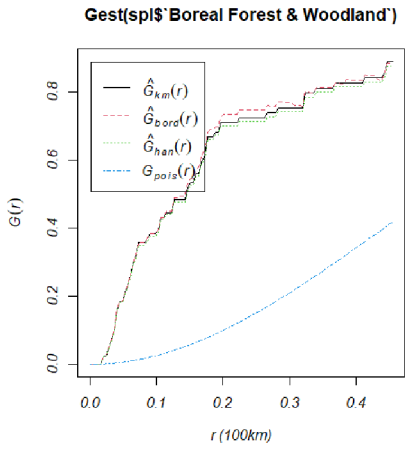

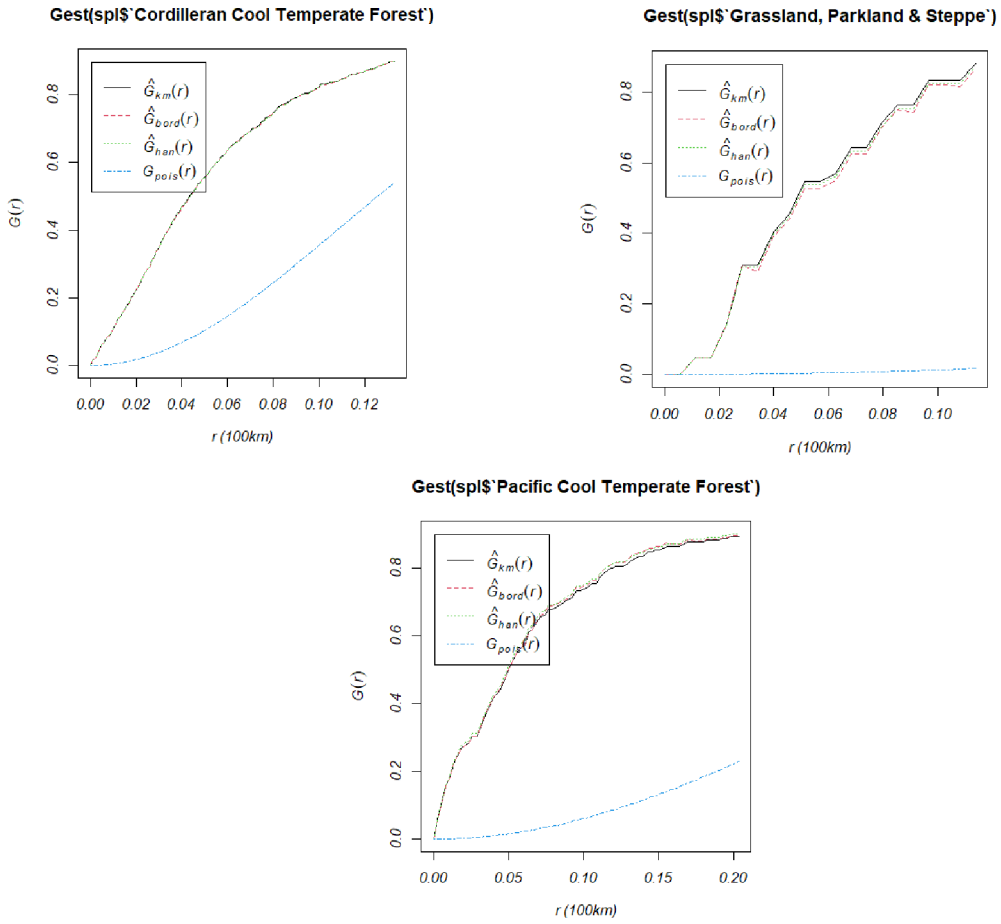

Figures 35 – 39: Calculated G-function (interaction with vegetation zones). Source: own data processing.

The G-function was as well calculated for the rest of the covariates. Graphs on Figures 40 – 45 show the calculated values of $\hat{G}(r)$ and $G_{pois}(r)$ for average drought levels factor. The result suggests a correlation between wildfires and each drought levels ($\hat{G}(r) > G_{pois}(r)$).

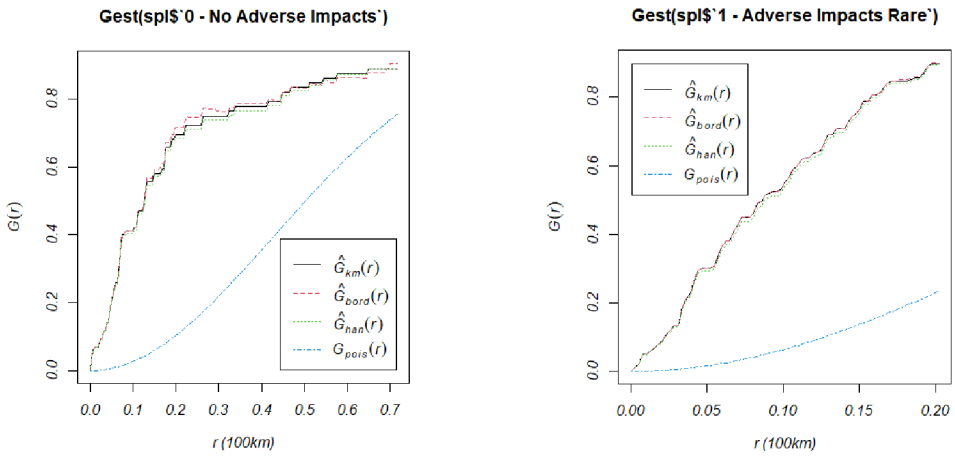

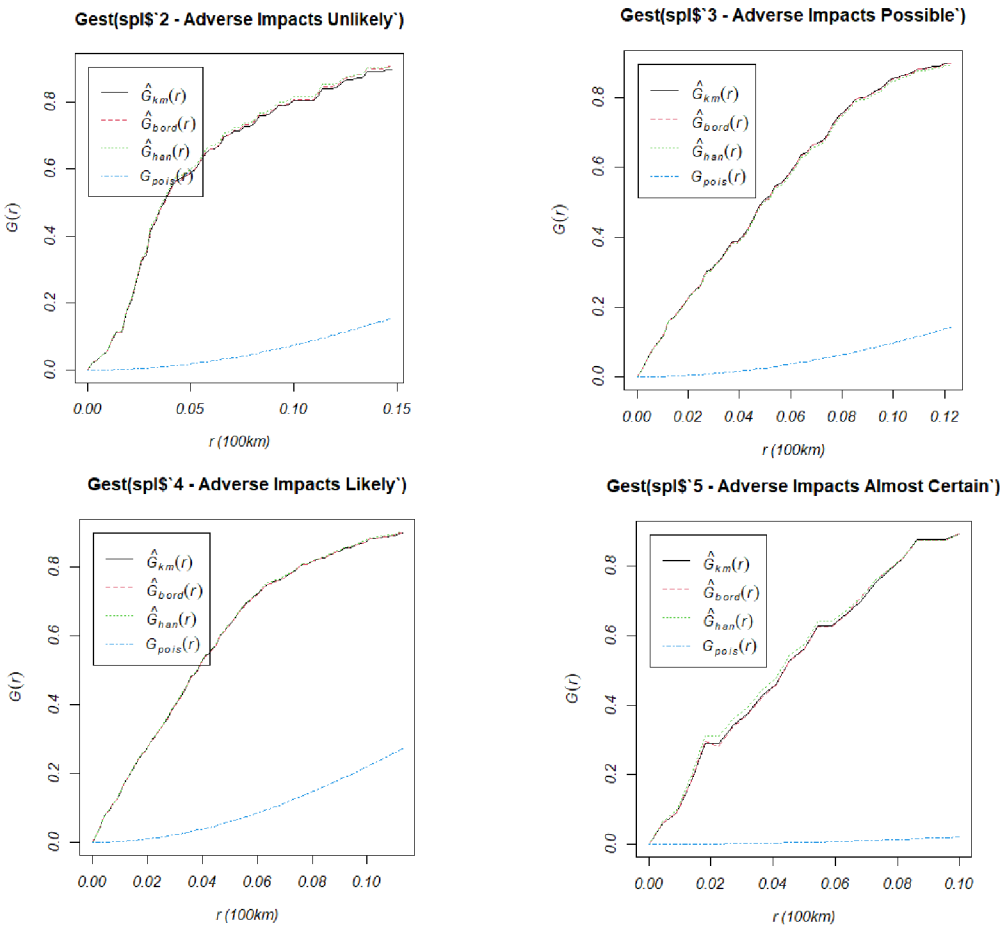

Figures 40 – 45: Calculated G-function (interaction with average drought level). Source: own data processing.

Due to the fact that covariate distance from road is a continuous variable it was converted to categorical using ranges of distances. The used brakes for the ranges were: 0 m, 7 000 m, 20 000 m, 100 000 m, and 180 000 m. The resulted G functions are shown on Figures 46 – 50.

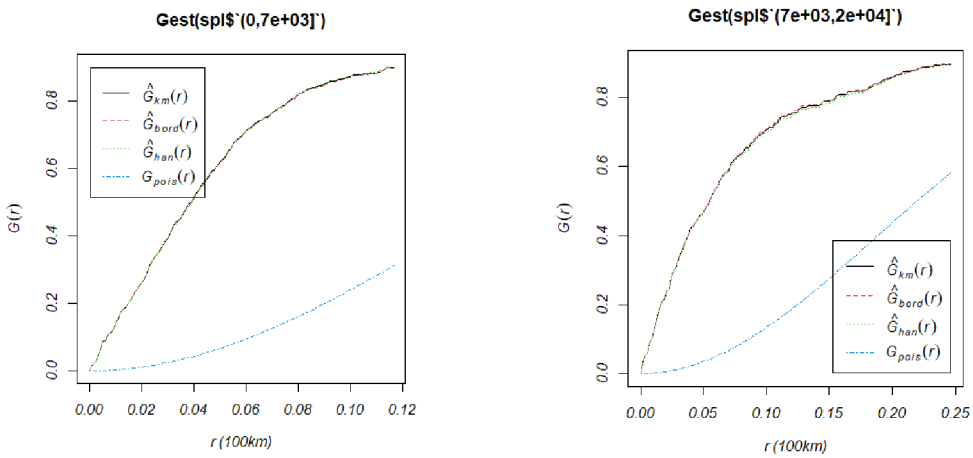

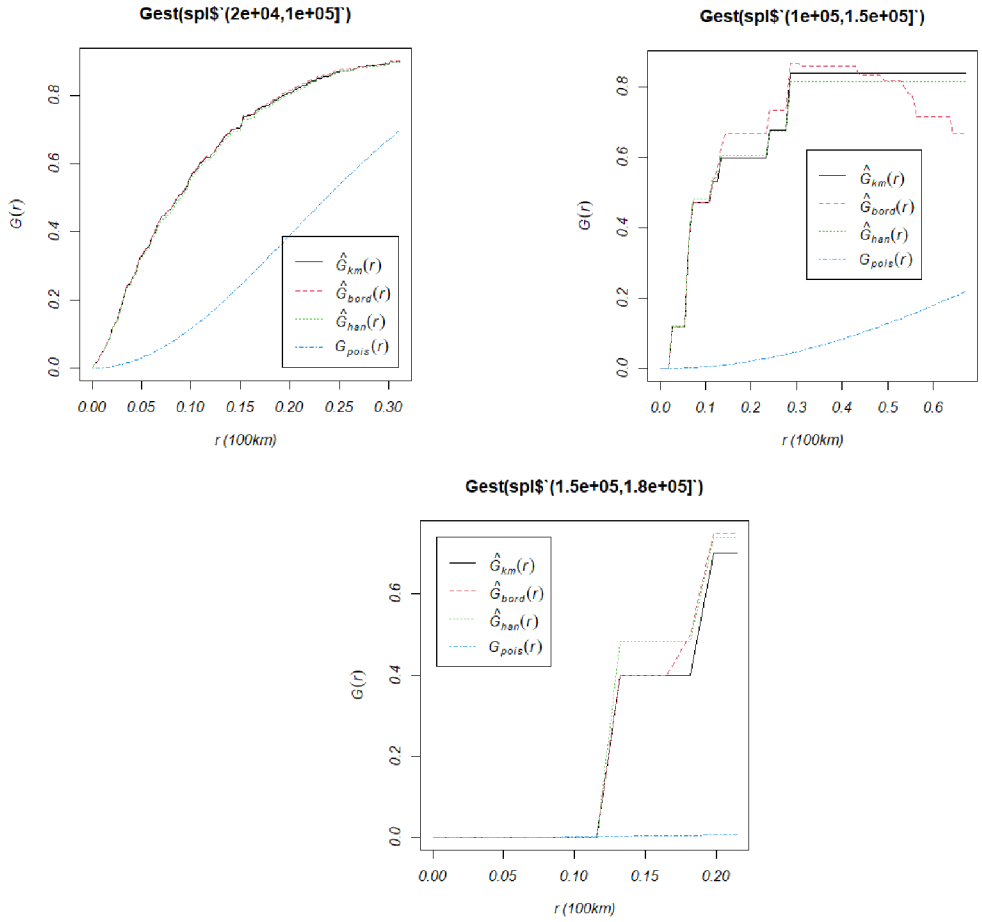

Figures 46 – 50: Calculated G-function (interaction with distance from roads). Source: own data processing.

The graphs show the interaction between wildfires and distance from roads at different ranges. It is visible that the values of $\hat{G}(r)$ are smaller than and $G_{pois}(r)$ on the last Figure (range from 150 000 m to 180 000 m) suggesting correlation between data.

G-function was calculated to assess interaction between mean wind speed and wildfires in terms of 2nd order effect. The results are shown in Figures 51 – 54. Since mean wind speed is a continuous variable 4 ranges were used to visualize the interaction between wildfires and the factor. The used ranges were calculated automatically in R using the following breaks: 1.31 m/s, 3.82 m/s, 6.32 m/s, 8.82 m/s, and 11.3 m/s.

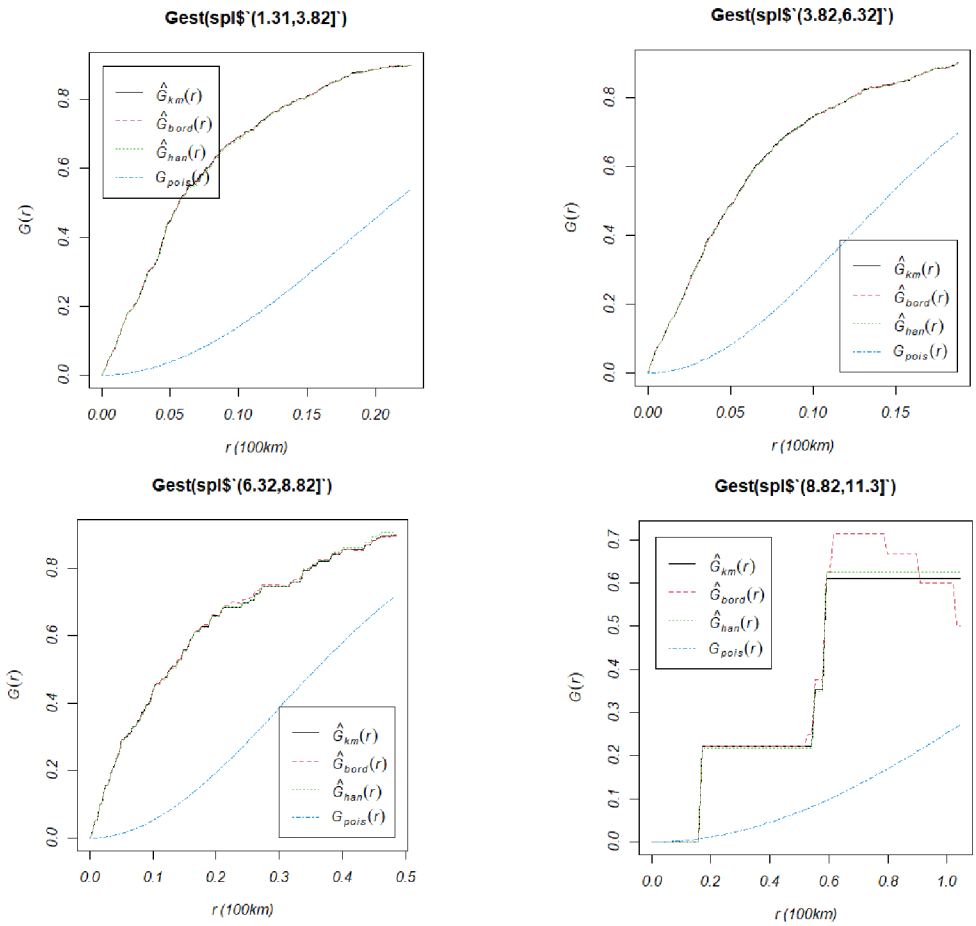

Figures 51 – 54: Calculated G-function (interaction with mean wind speed). Source: own data processing.

The curves of $\hat{G}(r)$ suggest that there is a correlation between this factor and wildfires.

5.3 Modeling wildfire distribution

5.3.1 Mean wind speed

A Poisson point process model was used to model a relationship between external factors (wind speed, distance from closest roads, vegetation zones, drought level) and wildfire events point pattern. A plot in Figure 55 shows the relationship between the annual mean wind speed and wildfires that occurred during the wildfire season.

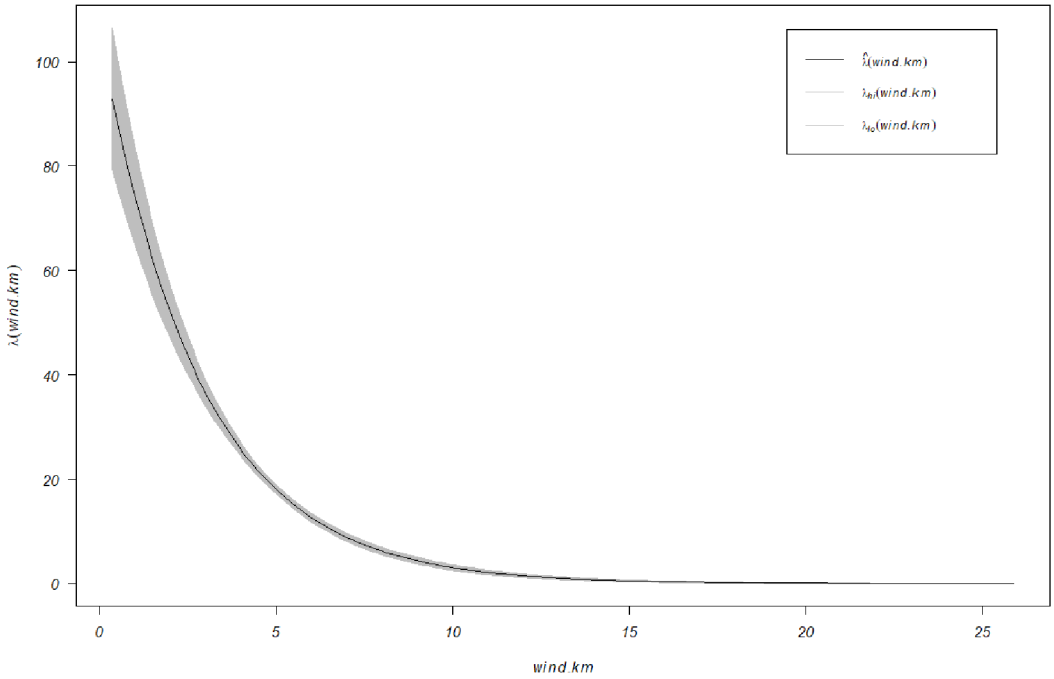

Figure 55: Fitted Poisson point process model: relationship between wildfire density and annual mean wind speed. Source: own data processing.

The plot suggests a decreasing relationship between the annual mean wind speed and the wildfires. The parameters of the model can be observed in Figure 56.

```
Nonstationary Poisson process

Log intensity:  ~wind.km

Fitted trend coefficients:
(Intercept)     wind.km
  4.6636741  -0.3534561

             Estimate       S.E.    CI95.lo    CI95.hi Ztest      Zval
(Intercept)  4.6636741 0.07875080  4.5093254  4.8180229   ***  59.22066
wind.km     -0.3534561 0.01616016 -0.3851295 -0.3217828   *** -21.87207
Problem:
 Values of the covariate 'wind.km' were NA or undefined at 0.03% (2 out of 6158) of the quadrature points
```

Figure 56: Annual mean wind speed model parameters. Source: own data processing.

Value of the Akaike information criterion for this model was -6881.031. If we take an equation (1) described in section 4.3.1, the model will take the following form:

$$\lambda(i) = e^{4.66-0.35(\text{logged annual mean wind speed})} \quad (4)$$

This can be interpreted as for every unit increase in the annual mean wind speed the wildfire density will decrease by $e^{-0.35}$ or by ~0.705. The effect of the covariate was tested afterward. The resulting model was compared to the null model (homogeneous distribution across the study area). Therefore, the question for the

comparison is whether the model included an external factor better predicts the wildfire density than the null model.

```
Analysis of Deviance Table

Model 1: ~1      Poisson
Model 2: ~wind.km        Poisson
  Npar Df Deviance  Pr(>Chi)
1    3
2    4  1   549.64 < 2.2e-16 ***
---
Signif. codes:  0 ‘***’ 0.001 ‘**’ 0.01 ‘*’ 0.05 ‘.’ 0.1 ‘ ’ 1
```

Figure 57: Comparison of null and annual mean wind speed model. Source: own data processing.

According to the output in Figure 57, the model of annual mean wind speed predicts the wildfire density better than the null model. Hence, the null model is rejected (p-value < 0.05).

Other Poisson point process models were fitted to explore the relationship between the annual mean wind speed and wildfire events that occurred in April (the beginning of the wildfire season), July (the peak of the wildfire season), and September (the end of the wildfire season). The relationship between the factor and wildfires can be observed in Figures 58 – 60.

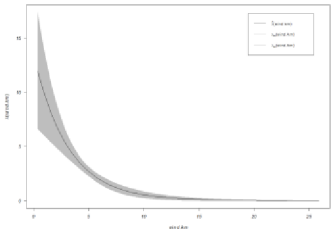

April

```
Fitted trend coefficients:
(Intercept)     wind.km
  2.6038150  -0.3230861
```

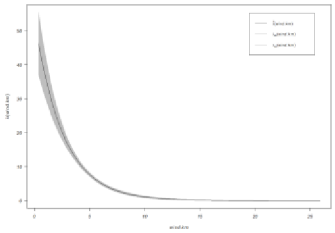

July

```
Fitted trend coefficients:
(Intercept)     wind.km
  3.9786468  -0.3880805
```

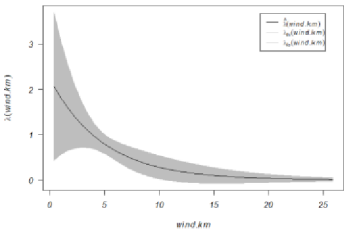

September

```
Fitted trend coefficients:
(Intercept)     wind.km
  0.8021569  -0.2065853
```

Figures 58 – 60: The relationship between wildfire density and annual mean wind speed during April, July and September. Source: own data processing.

The resulted fitted models showed the decreasing relationship between the factor and wildfire density that occurred in April and July. Although the model fitted for September wildfire events showed a less significant relationship between the annual wind speed and wildfire density, the null model was still rejected (p-value = 0.009).

5.3.2 Distance from roads

Proximity to the roads was chosen as a proxy of anthropogenic activity effect on the wildfire occurrence in British Columbia. It was discovered that 50% of the wildfire events occurred at the distance less than 7 kilometers from the closest road. Figure 61 shows the distinguishing of wildfires according to distance ranges.

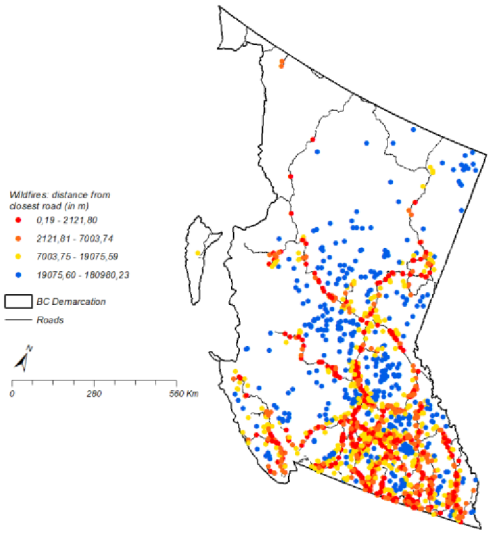

Figure 61: Visualization of the distance from wildfires to the closest road. Source: own data processing

The model fitted to the relationship between the distance from roads and wildfire events for the whole wildfire season had the following parameters:

```
Nonstationary Poisson process

Log intensity:  ~roads.km

Fitted trend coefficients:
  (Intercept)      roads.km
 3.946371e+00 -4.202494e-05

                 Estimate         S.E.        CI95.lo       CI95.hi Ztest      Zval
(Intercept)  3.946371e+00 3.339152e-02  3.880925e+00  4.011817e+00   *** 118.18484
roads.km    -4.202494e-05 1.515228e-06 -4.499473e-05 -3.905514e-05   *** -27.73507
Problem:
 Values of the covariate 'roads.km' were NA or undefined at 1.8% (110 out of 6158) of the quadrature points
```

Figure 62: Distance from roads model parameters. Source: own data processing.

The summary of the model (Figure 62) and plot in Figure 63 conclude that the relationship between the covariate and the point pattern is decreasing – the wildfire density will decrease with every unit increase in the distance from the road. The null model was rejected (p-value < 0.05). The AIC value for this model was -7837.655. This AIC is lower than the AIC for the previous model (mean wind speed). This means that distance from roads factor better explains the distribution of wildfire incidents that occurred in British Columbia during the 2021 wildfire season.

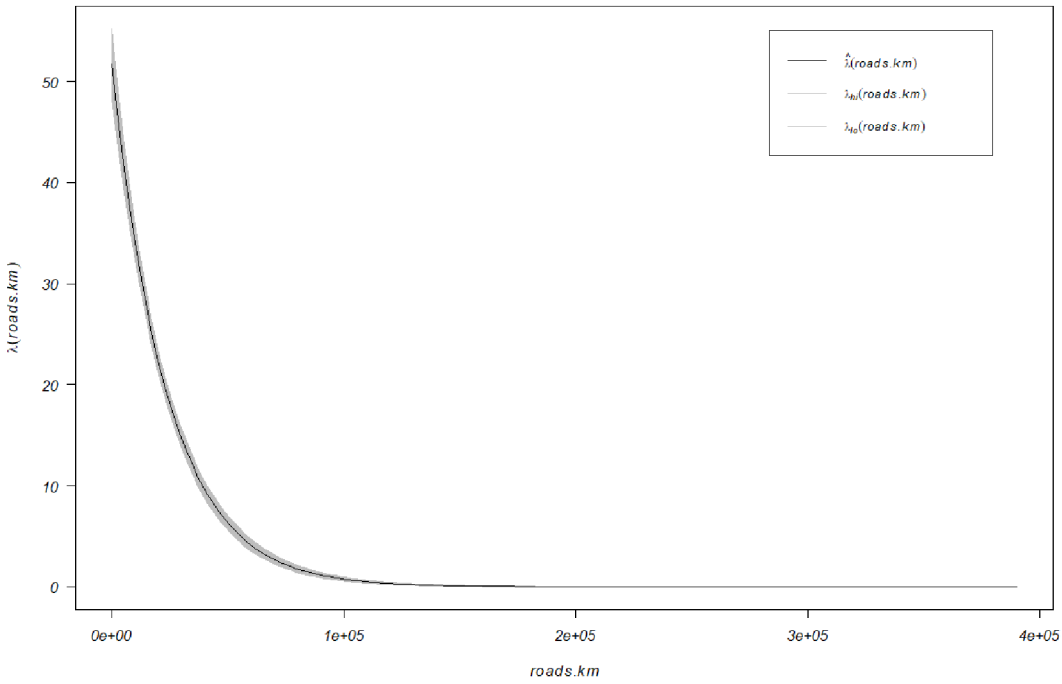

Figure 63: Fitted Poisson point process model: relationship between wildfire density and distance from roads. Source: own data processing.

The Poisson point process was fitted to model the relationship between the distance from roads and wildfire point patterns during April, July, and September. Plots depicted in Figures 64 - 66 visualize the relationship. All three models were compared to the null model. As a result, the null model was rejected in all three cases (p-value < 0.05).

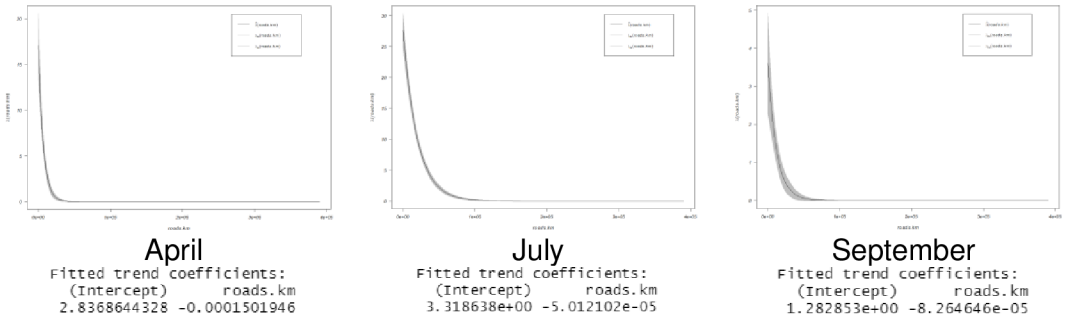

Figure 64 – 66: The relationship between wildfire density and distance from roads during April, July and September. Source: own data processing.

5.3.3 Vegetation zones

As was described in contributing factors section this covariate is a categorical variable that consists of 5 levels (vegetation zones). The absolute majority of wildfires occurred in the Cordilleran Cool Temperate Forest zone – 80% of the total number of wildfires. The lowest number of wildfires was recorded in Alpine Tundra – only 2 events. Wildfire counts and percentages within the rest of the vegetation zones are shown in Figure 67.

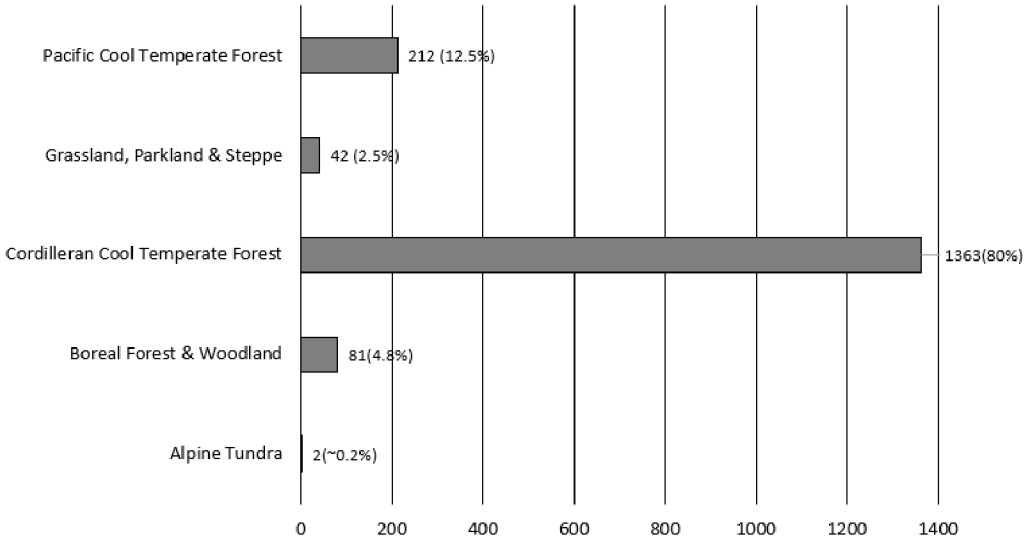

Figure 67: Number of wildfires in different vegetation zones during the 2021 wildfire season. Source: own data processing.

As it was mentioned above this covariate represents a categorical variable. In this case, Poisson point process model should be adjusted – vegetation zones will be specified as a factor. The parameters of the fitted model are shown in Figure 68. The model output suggests that the effect of vegetation zone 1 (Alpine Tundra) is not significant. At the same time, the rest of the vegetation zones showed a significant influence on wildfire patterns.

```
Nonstationary Poisson process

Log intensity:  ~factor(v.km)

Fitted trend coefficients:
  (Intercept) factor(v.km)2 factor(v.km)3 factor(v.km)4 factor(v.km)5
   -0.5162287     1.7610508     3.9751058     2.9876407     5.3489954

                Estimate      S.E.    CI95.lo   CI95.hi Ztest      Zval
(Intercept)   -0.5162287 0.3535534 -1.209181 0.1767232       -1.460115
factor(v.km)2  1.7610508 0.3719319  1.032078 2.4900239   ***  4.734875
factor(v.km)3  3.9751058 0.3545955  3.280111 4.6701003   *** 11.210254
factor(v.km)4  2.9876407 0.3601012  2.281855 3.6934261   ***  8.296670
factor(v.km)5  5.3489954 0.3818813  4.600522 6.0974689   *** 14.006959
Problem:
 Values of the covariate 'v.km' were NA or undefined at 1.1% (70 out of 6158) of the quadrature points
```

Figure 68: Vegetation zones model parameters. Source: own data processing.

Other models were fitted to explore the relationship between the vegetation zones and wildfires during April, July, and September. The output from the model suggested that the effect of the vegetation zones on wildfire distribution during April and September was not significant. At the same time, the effect of three vegetation zones is considered significant during July. These vegetation zones are Cordilleran Cool Temperate Forest, Grassland, Parkland & Steppe, and Pacific Cool Temperate Forest. Parameters of the model are shoiwn in Figure 69.

```
Nonstationary Poisson process

Log intensity:  ~factor(v.km)

Fitted trend coefficients:
  (Intercept) factor(v.km)2 factor(v.km)3 factor(v.km)4 factor(v.km)5
    -0.628009      0.123996      3.394496      2.072857      4.832208

                Estimate      S.E.     CI95.lo   CI95.hi Ztest       Zval
(Intercept)   -0.628009 0.4472136 -1.5045316 0.2485135       -1.4042709
factor(v.km)2  0.123996 0.5577734 -0.9692197 1.2172117        0.2223053
factor(v.km)3  3.394496 0.4488572  2.5147517 4.2742394   ***  7.5625295
factor(v.km)4  2.072857 0.4618802  1.1675881 2.9781252   ***  4.4878663
factor(v.km)5  4.832208 0.5026247  3.8470819 5.8173344   ***  9.6139490
```

Figure 69: Vegetation zones model parameters for July. Source: own data processing.

The value of the AIC for this model was -7663.731. This value is higher than the AIC value for the distance from the roads model. However, it is lower than the AIC value of the first model (mean wind speed).

5.3.4 Average drought level

Summary statistics for wildfire events according to drought levels were calculated. According to the plot in Figure 70 the majority (~ 70%) of the wildfires occurred within the regions where the average drought level was higher than 3 during the 2021 wildfire season. A map visualizing the approximate distribution of the average drought level can be found in section 4.2.2.

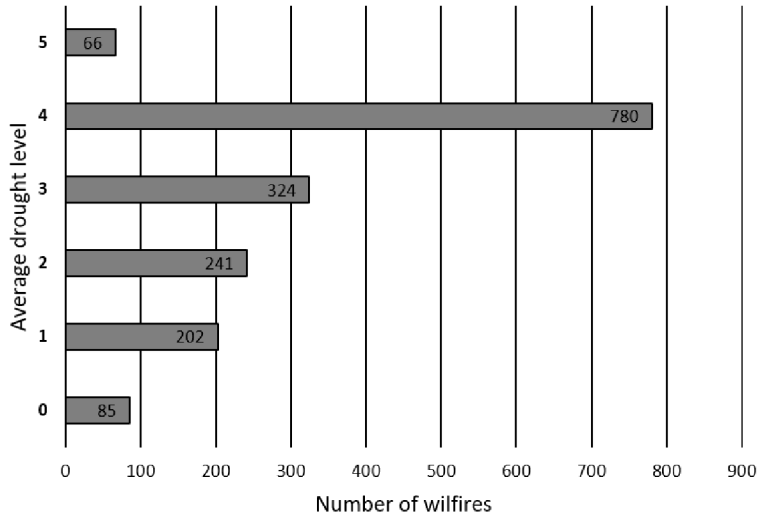

Figure 70: Number of wildfires in relation to average drought level. Source: own data processing.

The Poisson point process was fitted to model the relationship between wildfire density and the average drought level. The fitted model showed an increasing relationship between the variables. This relationship is depicted in Figure 71. Subsequently, the fitted model was compared to the null model using the likelihood ratio test. On the basis of the p-value (< 0.05), the null model was rejected. The fitted Poisson point process model predicts the density of wildfires better than the null model.

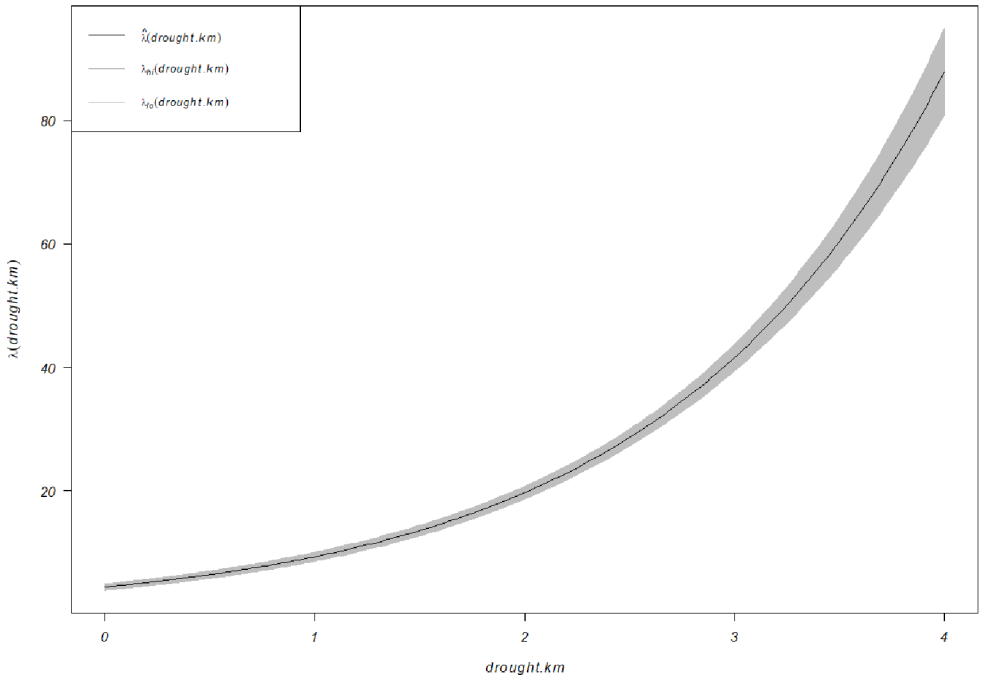

Figure 71: Fitted Poisson point process model: relationship between wildfire density and average drought level. Source: own data processing.

The Akaike information criterion for this model was -7885.654. This is the lowest value of the AIC between the four models.

Three more models were fitted to wildfire events that occurred in April, July, and September separately. The comparison of the trends and coefficients of the models is shown in Figures 72 – 74. There is an increasing trend of wildfire density in relation to the average drought level in all three cases. The fitted models were subsequently compared to the null model. The null model was rejected based on small p-values.

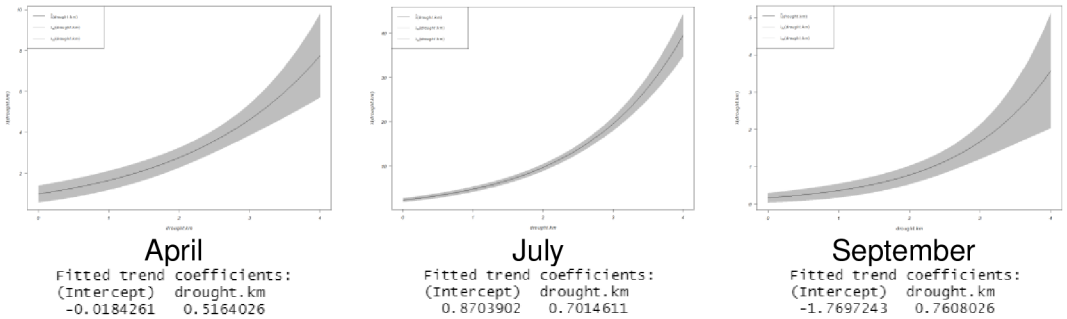

Figures 72 – 74: The relationship between wildfire density and average drought level during April, July and September. Source: own data processing.

5.3.5 All covariates included model

Another Poisson point process was fitted to model the relationship between the density of wildfires during the whole wildfire season and all the covariates. The parameters of the all covariates included model are shown in Figure 75.

```
Nonstationary Poisson process

Log intensity:  ~factor(v.km) + drought.km + wind.km + roads.km

Fitted trend coefficients:
  (Intercept) factor(v.km)2 factor(v.km)3 factor(v.km)4 factor(v.km)5    drought.km       wind.km      roads.km
 1.166649e+00  1.586784e+00  2.617325e+00  1.804377e+00  3.359119e+00  4.208189e-01 -1.284571e-01 -2.782058e-05

                  Estimate         S.E.       CI95.lo       CI95.hi Ztest       Zval
(Intercept)    1.166649e+00 3.769791e-01  4.277831e-01  1.905514e+00    **   3.094730
factor(v.km)2  1.586784e+00 3.746316e-01  8.525194e-01  2.321048e+00   ***   4.235585
factor(v.km)3  2.617325e+00 3.569367e-01  1.917742e+00  3.316908e+00   ***   7.332742
factor(v.km)4  1.804377e+00 3.636382e-01  1.091660e+00  2.517095e+00   ***   4.962013
factor(v.km)5  3.359119e+00 3.849930e-01  2.604547e+00  4.113691e+00   ***   8.725144
drought.km     4.208189e-01 2.631590e-02  3.692407e-01  4.723971e-01   *** 15.991053
wind.km       -1.284571e-01 1.722937e-02 -1.622260e-01 -9.468813e-02   *** -7.455705
roads.km      -2.782058e-05 1.493427e-06 -3.074765e-05 -2.489352e-05   *** -18.628691
Problem:
 Values of the covariates 'v.km', 'drought.km', 'wind.km', 'roads.km' were NA or undefined at 5.6% (344 out of 6158) of the quadrature
points
```

Figures 75: All covariates included model parameters. Source: own data processing.

According to the parameters of the model, all the covariates significantly influence the distribution of wildfire incidents in British Columbia during the 2021 wildfire season. The 'Zval' field shows how the distance influences the intensity of wildfires. The higher influence results in a higher value of Z. The negative and positive signs of Z indicate the type of influence. In this case, it is evident that distance from the roads and drought levels have a more substantial influence on wildfires. Drought levels have a positive influence, while the distance from roads has a negative influence respectively.

Alternative models were created by extracting different coefficients one by one for future comparison. All the models were subsequently compared using the Akaike information criterion (AIC).

Model	**AIC value**
All covariates included	-9010.31
Excluded vegetation type	-8679.674
Excluded mean wind speed	-8953.172
Excluded distance from roads	-8504.821
Excluded average drought level	-8758.737

Table 3: Comparison of the models based on the AIC. Source: own data processing.

Based on the values of the AIC values from Table, 3 the best model is the model that included all the factors. The fitted trend of this model is depicted in Figure 76.

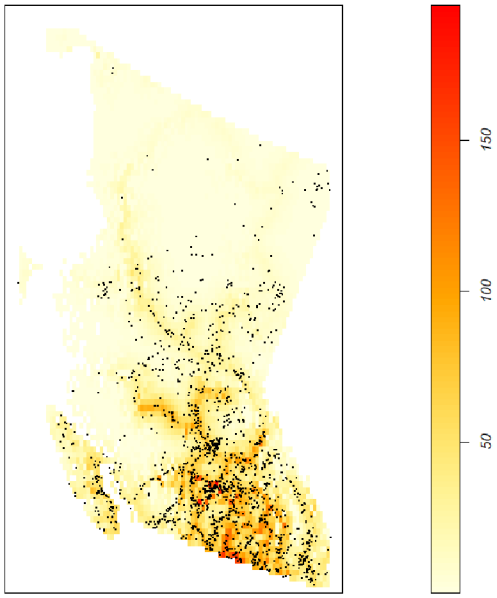

Figure 76: Fitted trend of wildfire density (all covariates). Source: all data processing.

As it can be seen from Figure 76 the highest wildfire density occurs in the southern part of British Columbia. At the same time, moderate wildfire density also appears in the center of the province. This model was subsequently used to predict the trend of wildfires in British Columbia. The predicted values were plotted using a perspective plot and can be observed in Figure 77.

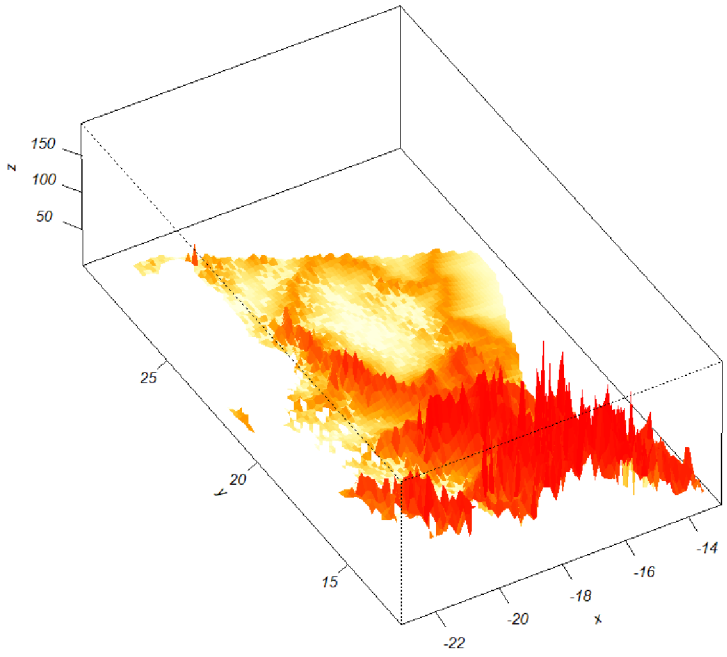

Figure 77: Visualization of the predicted trend of the wildfire density based on the all covariates included model. Source: own data processing.

5.3.6 Comparison with the wildfires data from 2022 wildfire season

The final model's (all covariates included) prediction of wildfire distribution was compared to the distribution of wildfire incidents during the 2022 wildfire season. In total 1 758 wildfire incidents were recorded during the 2022 wildfire season that resulted in almost 133 500 ha of area burned. (Province of British Columbia, 2022). Figure 78 shows the locations of 2022 wildfires overlay with the final model predictions.

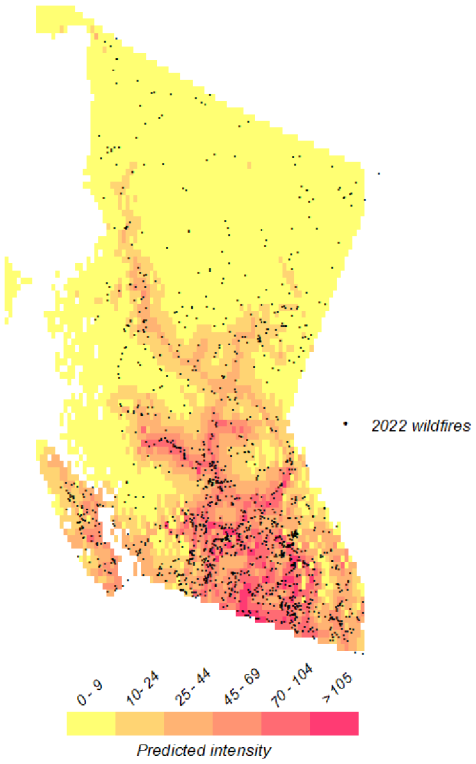

Figure 78: Overlay of the prediction and locations of 2022 wildfires. Source: wildfires - B.C.'s Map Hub, 2023; own data processing.

Table 4 shows the total number of wildfires that occurred inside the predicted higher-risk zones. In total, 790 wildfires occurred in the higher-risk zones (intensity greater than 45). This represents ~51% of the total wildfires that occurred in 2022. 571 wildfires occurred within the moderate risk zones (intensity between 10 and 45), ~ 37% of all wildfires. In the lower-risk zones (less than 10) occurred 200 (~13%) wildfires in 2022.

Predicted intensity	Number of 2022 wildfires
0 – 9	200
10 – 24	213
25 – 44	358
45 – 69	375
70 – 104	343
> 105	72

Table 4: Total number of wildfires occurred within the risk zones. Source: own data processing.

6. Discussion

It is obvious from the results that the resulting pattern of wildfire events is clustered in terms both of 1st order and 2nd order effects. The clustering was mainly observed in the southern and central parts of British Columbia regardless of the studied month. As for the K- (L-) functions, the results showed that the data were exhibiting clustering at all distances. As for the G-function, the correlation was observed in terms of each external factor. The exceptions are the Alpine Tundra vegetation zone, wind speed greater than 8.8 m/s, and longer distances from the roads (> 150 000 m). The absence of correlation with Alpine Tundra was probably due to the low number of wildfires (two) recorded within this vegetation zone.

The author of the diploma thesis modeled the distribution of wildfires considering the possible influence of external factors. The final model was chosen based on the value of AIC and included all the external factors. It is evident from the model's output that the distance from the roads and drought levels have a major influence on wildfire intensity among all the factors. The importance of distance from roads for wildfire distribution was also posited in research conducted by Aragó et al. At the same time, roads strongly influenced human-caused wildfires, while the water deficiency factor showed the strongest influence for lightning-caused wildfires (Yang et al., 2015). These results correlate with the results presented in this diploma thesis. Predictions based on the final model were subsequently compared to the wildfire records from the 2022 wildfire season. The locations of 2022 wildfires follow the outlines of the predictions.

This research represents one of the examples of how point pattern analysis can be implemented for wildfire studies. External factors provide valuable information on wildfire risk in the area, which is crucial for wildfire management. For future research, detailed information on wind speed (current wind speed at the time of the wildfires) might improve the output of the final model. Other studies also consider temperature, relative humidity, elevation, land use, and the cause of wildfires in their computations (Aftergood & Flannigan, 2022; Aragó et al., 2016; Yang et al., 2015). Since lightning is associated with ~ 60% of ignitions (Province of British Columbia, 2022), further research can include thunderstorm activities and lightning density in calculations.

Considering Canadian wildfire management recognizes a review of previous wildfires phase as a separate phase (mentioned in section 3.6.1), the results obtained from the 1st and 2nd order effect analysis already serve as a reference for future management recommendations. The prediction of the final model could serve as a fire risk map of the region. This kind of map could be taken into consideration during the decision-

making process of wildfire managers. Areas of higher wildfire risk might receive enhanced resources, firefighting staff, and funding. Point process modeling also helps to analyze the influence of external factors (as distance from roads or drought levels) on wildfire distribution allowing more effective prevention and preparedness for wildfires.

Another opportunity for this research can be climate change problematics. As was discussed in section 3.4, climate change creates warmer and drier conditions leading to decreased fuel moisture. The ongoing climate change will impact the patterns of wildfire seasons. Therefore, further monitoring of climate change, annual analyses of wildfire incidents, and identifying associated factors are critical elements for understanding wildfire behavior under changing climate. However, this cannot be done without proper and available datasets.

Data availability and data quality are crucial for point pattern analysis. Thus, mapping wildfires should be done on a regular basis, and each incident should include as much detailed information as possible. One of the disadvantages of the dataset used in the analyses is that it did not have information on the source of the ignition. The source of the wildfire is crucial for wildfire risk mapping and further management, hence, the wildfire distribution for each cause should be considered and modeled separately. Nevertheless, the data analysis can be performed in RStudio, which is free and can be used by anyone. Due to this feature, point pattern methods are widely accessible and can be implemented while developing wildfire management strategies.

7. Conclusion

This diploma thesis intended to examine the pattern of wildfire events that occurred in 2021 in British Columbia in terms of 1st order and 2nd order effects. An additional aim was to model the wildfire distribution across the area. The calculations considered four external factors of possible influence on wildfire: mean wind speed, distance from roads, vegetation zones, and average drought level. A detailed description of the wildfire problematics, methodology, study area, and results are presented in their respective sections. The discovered pattern of wildfires was clustering, with significant densities occurring in the central and southern parts of the study region. The final model outputs suggest that distance from roads and average drought levels influence wildfire intensity the most. Predictions based on the final model define the locations of wildfires that occurred one year later.

This thesis serves as an example of application point pattern methodology for the study and understanding of wildfire distribution. It has to be mentioned that such variables as the information on wind speed during the wildfire localization might improve the model's output. Nevertheless, the final deliverables of the research may serve as a wildfire risk map for the study area.

8. Bibliography

Aftergood, O. S. R., & Flannigan, M. D., 2022. Identifying and analyzing spatial and temporal patterns of lightning-ignited wildfires in Western Canada from 1981 to 2018. Canadian Journal of Forest Research, 52(11), 1399–1411.

Alaska Wildland Fire Coordinating Group, 2015. Wildland Fire Guide. Alaska. Available at: https://forestry.alaska.gov/Assets/pdfs/fire/assignments/2016%20Alaska%20Wildland%20Fire%20Guide.pdf

Amiro, B. D., Stocks, B. J., Alexander, M. E., Flannigan, M. D., & Wotton, B. M., 2001. Fire, climate change, carbon and fuel management in the Canadian boreal forest. International Journal of Wildland Fire, 10(3–4), 405–413.

Aragó, P., Juan, P., Díaz-Avalos, C., & Salvador, P., 2016. Spatial point process modeling applied to the assessment of risk factors associated with forest wildfires incidence in Castellón, Spain. European Journal of Forest Research, 135(3), 451–464. https://doi.org/10.1007/s10342-016-0945-z

Baddeley, A., 2007. Spatial Point Processes and their Applications. In: Weil, W. (eds) Stochastic Geometry. Lecture Notes in Mathematics, vol 1892. Springer, Berlin, Heidelberg.

Baddeley, A., 2010. Analysing spatial point patterns in R. ©CSIRO and University of Western Australia

Badmaev, N., Bazarov, A., Kulikov, A., Gyninova, A., Sympilova, D., Shakhmatova, E., Badmaeva, N., Gonchikov, B. M., & Mangataev, A., 2019. Global climate change: Wild fires and permafrost degradation in the Republic of Buryatia (Eastern Siberia, Russia). IOP Conference Series: Earth and Environmental Science, 320(1).

Baldwin, K., Allen, L., Basquill, S., Chapman, K., Downing, D., Flynn, N., MacKenzie, W., Major, M., Meades, W., Meidinger, D., Morneau, C., Saucier, J-P., Thorpe, J., Uhlig, P, 2020. Vegetation Zones of Canada: a Biogeoclimatic Perspective. Natural Resources Canada, Canadian Forest Service. Great Lake Forestry Center, Sault Ste. Marie, ON, Canada.

B.C.’s Map Hub, 2023. Fire Locations – Current View. ArcGIS Available at: https://governmentofbc.maps.arcgis.com/home/item.html?id=397a1defe7f04c2b8ef6511f6c087dbf

Bonan, G. B., & Shugart, H. H., 1989a. ENVIRONMENTAL FACTORS AND ECOLOGICAL PROCESSES IN BOREAL FORESTS. In Annu. Rev. Ecol. Syst (Vol. 20).

Brown, T., Clyne, O., Pletcher, E., 2021. Spatial point process models in R. Available at: https://kevintshoemaker.github.io/NRES-746/sppm.html

Canadian Council of Forest Ministers, 2021. Action Plan 2021 – 2026: A Roadmap for Implementing the Canadian Wildland Fire Strategy Using a Whole-of-Government. Ontario, Canada. Available at: https://www.ccfm.org/releases/wildland-fire-management-working-group-action-plan-2021-2026/

Coogan, S. C. P., Aftergood, O., & Flannigan, M. D., 2022. Human- and lightning-caused wildland fire ignition clusters in British Columbia, Canada. International Journal of Wildland Fire.

de Groot, W. J., Flannigan, M. D., & Cantin, A. S., 2013. Climate change impacts on future boreal fire regimes. Forest Ecology and Management, 294, 35–44.

Gauthier, S., Bernier, P., Kuuluvainen, T., Shvidenko, A. Z., & Schepaschenko, D. G., 2015. Boreal forest health and global change.

Girardin, M. P., Ali, A. A., & Hély, C., 2010. Wildfires in boreal ecosystems: Past, present and some emerging trends. In International Journal of Wildland Fire (Vol. 19, Issue 8, pp. 991–995).

Government of Canada. 2015. Introduction – British Columbia. Natural Resources Canada. Gouvernement du Canada. Available at: https://www.nrcan.gc.ca/changements-climatiques/impacts-adaptation/introduction-british-columbia/10395 (Accessed: December 15, 2022)

Government of Canada, n.d. Canadian Forest Fire Weather Index (FWI) System. Natural Resources Canada. Gouvernement du Canada. Available at: https://cwfis.cfs.nrcan.gc.ca/background/summary/fwi?wbdisable=true

Grekousis, G, 2020. Spatial Analysis Methods and Practice: Describe – Explore – Explain through GIS. Cambridge: Cambridge University Press.

Haghani, M., Kuligowski, E., Rajabifard, A., & Kolden, C. A., 2022. The state of wildfire and bushfire science: Temporal trends, research divisions and knowledge gaps. Safety Science, 153.

Hansen, M. C., Potapov, P. V., Moore, R., Hancher, M., Turubanova, S. A., Tyukavina, A., et al, 2013. High-Resolution Global Maps of 21st-Century Forest Cover Change. Science 342, 850–853.

Hoffman, K. M., Christianson, A. C., Gray, R. W., & Daniels, L., 2022. Western Canada's new wildfire reality needs a new approach to fire management. Environmental Research Letters, 17(6).

International Arctic Research Center, 2020. Alaska's Changing Wildfire Environment. International Arctic Research Center. Alaska. Available at: https://uaf-iarc.org/alaskas-changing-wildfire-environment/

Kasischke, E. S. et al. (eds.), 2000. Fire, Climate Change, and Carbon Cycling in the Boreal Forest © Springer-Verlag New York, Inc.

Kasischke, E. S., Verbyla, D. L., Rupp, T. S., McGuire, A. D., Murphy, K. A., Jandt, R., Barnes, J. L., Hoy, E. E., Duffy, P. A., Calef, M., & Turetsky, M. R., 2010. Alaska's changing fire regime - implications for the vulnerability of its boreal forestsspi_sup1spii_sup. Canadian Journal of Forest Research, 40(7), 1313–

Khakzad, N., 2019. Modeling wildfire spread in wildland-industrial interfaces using dynamic Bayesian network. Reliability Engineering and System Safety, 189, 165–176.

Kim, J.-S., Kug, J.-S., Jeong, S.-J., Park, H., & Schaepman-Strub, G., 2020. Extensive fires in southeastern Siberian permafrost linked to preceding Arctic Oscillation.

Kim, S. J., Lim, C. H., Kim, G. S., Lee, J., Geiger, T., Rahmati, O., Son, Y., & Lee, W. K., 2019. Multi-temporal analysis of forest fire probability using socio-economic and environmental variables. Remote Sensing, 11(1).

Li, X. Y., Jin, H. J., Wang, H. W., Marchenko, S. S., Shan, W., Luo, D. L., He, R. X., Spektor, V., Huang, Y. D., Li, X. Y., & Jia, N., 2021. Influences of forest fires on the permafrost environment: A review. In Advances in Climate Change Research (Vol. 12, Issue 1, pp. 48–65). National Climate Center.

MacCarthy, J., Weisse, M., Tyukavina., S, Harris, N., 2022. New Data Confirms: Forest Fires Are Getting Worse. World Resource Institute. Washington, DC. Available at: https://www.wri.org/insights/global-trends-forest-fires.

Macias Fauria, M., & Johnson, E. A., 2008. Climate and wildfires in the North American boreal forest. In Philosophical Transactions of the Royal Society B: Biological Sciences (Vol. 363, Issue 1501, pp. 2317–2327). Royal Society.

MacMillan, R., Sun, L., & Taylor, S. W., 2022. Modeling Individual Extended Attack Wildfire Suppression Expenditures in British Columbia. Forest Science, 68(4), 376–388.

McGee, T., McFarlane, B., & Tymstra, C., 2015. Wildfire: A Canadian Perspective. In Wildfire Hazards, Risks, and Disasters (pp. 35–58). Elsevier Inc.

NASA, 2021. Global Climate Change: How Do We Know Climate Change Is Real? The Earth Science Communications Team. Available at: https://climate.nasa.gov/evidence/

NASA, 2021. Global Climate Change: The Causes of Climate Change. The Earth Science Communications Team. Available at: https://climate.nasa.gov/causes/

Province of British Columbia, 2022. Statistics & Geospatial Data. Wildfire History. British Columbia, Canada. Available at: https://www2.gov.bc.ca/gov/content/safety/wildfire-status/about-bcws/wildfire-statistics

Province of British Columbia, 2022. Climate of B.C. Available at: https://www.welcomebc.ca/Choose-B-C/Explore-British-Columbia/Climate-of-B-C

Province of British Columbia, 2022 Wildfire season summary, Province of British Columbia. Canada. Available at: https://www2.gov.bc.ca/gov/content/safety/wildfire-status/about-bcws/wildfire-history/wildfire-season-summary

Province of British Columbia, 2022. British Columbia Drought Levels. ArcGIS. Available at: https://www.arcgis.com/home/item.html?id=4ca1ea286fc2474991822f42bdc45086

Richter, J., MacCarthy, J., Weisse, M., Tyukavina., S, 2022. Two Decades of Fire-Driven Loss in Unprecedented Detail. Global Forest Watch. Washington, DC: World Resources Institute. Available at: https://www.globalforestwatch.org/blog/data-and-research/trends-tree-loss-from-fires-unprecedented-detail/

Rowei, J. S., & Scotter, G. W., 1973. Fire in the Boreal Forest. In QUATERNARY RESEARCH (Vol. 3).

Scott, G. A. J., 1995. Canada's Vegetation: A World Perspective. McGill-Queen's University Press.

Schroeder, T. A., Wulder, M. A., Healey, S. P., & Moisen, G. G., 2011. Mapping wildfire and clearcut harvest disturbances in boreal forests with Landsat time series data. Remote Sensing of Environment, 115(6), 1421–1433.

Tchebakova, N. M., Parfenova, E., & Soja, A. J., 2009. The effects of climate, permafrost and fire on vegetation change in Siberia in a changing climate. Environmental Research Letters, 4(4).

Tomshin, O., & Solovyev, V., 2022. Features of the Extreme Fire Season of 2021 in Yakutia (Eastern Siberia) and Heavy Air Pollution Caused by Biomass Burning. Remote Sensing, 14(19).

Trancoso, R., Syktus, J., Salazar, A., Thatcher, M., Toombs, N., Wong, K. K. H., Meijaard, E., Sheil, D., & McAlpine, C. A., 2022. Converting tropical forests to agriculture increases fire risk by fourfold. Environmental Research Letters, 17(10).

Turner, R., 2009. Point patterns of forest fire locations. Environmental and Ecological Statistics, 16(2), 197–223.

Tymstra, C., Stocks, B. J., Cai, X., & Flannigan, M. D., 2020. Wildfire management in Canada: Review, challenges and opportunities. Progress in Disaster Science, 5.

Tyukavina, A., Potapov, P., Hansen, M. C., Pickens, A. H., Stehman, S. v., Turubanova, S., Parker, D., Zalles, V., Lima, A., Kommareddy, I., Song, X.-P., Wang, L., & Harris, N., 2022a. Global Trends of Forest Loss Due to Fire From 2001 to 2019. Frontiers in Remote Sensing, 3.

UCGIS, 2023. AM-07 - Point Pattern Analysis. UCGIS: GIS&T Body of Knowledge. Available at: https://gistbok.ucgis.org/bok-topics/point-pattern-analysis.

USDA, 2021. Climate Change and Wildfire in Alaska. U.S. Department of Agriculture. Washington DC. Available at: https://www.climatehubs.usda.gov/hubs/northwest/topic/climate-change-and-wildfire-alaska

Vadrevu, K. P., & Badarinath, K. V. S., 2009. Spatial pattern analysis of fire events in Central India - A case study. Geocarto International, 24(2), 115–131.

Walker, X. J., Baltzer, J. L., Cumming, S. G., Day, N. J., Ebert, C., Goetz, S., Johnstone, J. F., Potter, S., Rogers, B. M., Schuur, E. A. G., Turetsky, M. R., & Mack, M. C., 2019. Increasing wildfires threaten historic carbon sink of boreal forest soils. Nature, 572(7770), 520–523.

Wells, J. v., Dawson, N., Culver, N., Reid, F. A., & Morgan Siegers, S., 2020. The State of Conservation in North America's Boreal Forest: Issues and Opportunities. Frontiers in Forests and Global Change, 3.

Yang, J., Weisberg, P. J., Dilts, T. E., Loudermilk, E. L., Scheller, R. M., Stanton, A., Skinner, C., 2015. Predicting wildfire occurrence distribution with spatial point process models and its uncertainty assessment: a case study in the Lake Tahoe Basin, USA. International Journal of Wildland Fire. 24(3): 380-390. 11p.

Yu, Y., Dunne, J. P., Shevliakova, E., Ginoux, P., Malyshev, S., John, J. G., & Krasting, J. P., 2021. Increased risk of the 2019 Alaskan July Fires due to anthropogenic activity. Bulletin of the American Meteorological Society, 102(1), S1–S7.

Zyryanova, O. A., Milyutin, L. I., Muratova, E. N., Ryzhkova, V. A., Larionova, A. Y., Sedel'nikova, T. S., Korets, M. A., & Mikhailova, I. A, 2008. Boreal Forests of Siberia: Genetic, Species and Ecosystem Diversity.